Job copy

Limitations to Measuring Accuracy Inherent in the Laser Doppler Signal

by

William K. George, Jr.
State University of New York at Buffalo
Buffalo, NY 14214

0. Foreword

The laser Doppler anemometer (LDA) was conceived in the early 1960's with the pioneering work of Yeh and Cummins who first demonstrated that the Doppler shift of light caused by moving scatters could be detected by heterodyning the scattered light with a laser source on a photocell. In the last eleven years tremendous strides have been made toward making the LDA a reliable flow measuring instrument. Concurrent with the advances in LDA hardware has been considerable progress in understanding the fundamental properties of the LDA signals. It is the purpose of this paper to review that understanding as it relates to the properties of the ideal Doppler signal.

Understanding the ideal Doppler anemometer, divorced from hardware problems, is necessary to a proper evaluation of the real LDA. Only by recognizing and accounting for the inherent characteristics of the signal can a judgement of hardware performance be made.

The annoying characteristics of the ideal LDA that are presented in this paper should not be interpreted to discourage the potential user. On the contrary, the message of this paper is that the problems associated with signal interpretation have reached as state that can be described as "well understood". Moreover, for every problem that is presented, a solution or alternative approach is suggested! Nonetheless, the LDA, like any other sophisticated instrument, will never be an instrument for casual use by amateurs. If used, however, by careful experimentalists, cognizant of its peculiarities, it can in many experimental situations provide a uniquely non-intrusive and reliable flow measuring device.

This paper is based on the author's presentation at the LDA Symposium and the work that preceeded it. In the course of the symposium it became apparent that other researchers had independently reached similar conclusions. In

addition, several papers dealt with practical problems arising from characteristics of the non-ideal signals. Throughout this paper an attempt has been made to show how these contributions relate to the present work in an attempt to provide as useful a survey as possible. In no instance should these comments be substituted for a careful reading of these papers.

1. The Ideal Laser Doppler Anemometer

1.1 The Doppler Shift

The basic principal of the Doppler shift is illustrated in fig. 1. Radiation incident on a scattering center is reradiated or scattered at a different wave number. If $\underset{\sim}{k}_i$ is the wavenumber vector of the incident light and $\underset{\sim}{k}_s$ is the wavenumber of the scattered light, the difference wavenumber is given by

$$\underset{\sim}{K} = \underset{\sim}{k}_i - \underset{\sim}{k}_s \qquad 1.1.1$$

If $\underset{\sim}{u}$ is the velocity vector of the scattering center, the frequency shift between incident and scattered light as seen by a fixed observer is given by

$$\omega_D = 2\pi f_D = \underset{\sim}{K} \cdot \underset{\sim}{u} \qquad 1.1.2$$

If $\underset{\sim}{K}$ and $\underset{\sim}{u}$ are colinear as illustrated in the figure, the Doppler frequency difference is given by

$$\omega_D = 2\pi f_D = \frac{4\pi u}{\lambda_i} \sin\theta/2 \qquad 1.1.3$$

where λ_i is the wave length of the incident radiation.

It is clear from the fact that the Doppler frequency depends on the scalar product $\underset{\sim}{K} \cdot \underset{\sim}{u}$ that only the component of velocity parallel to $\underset{\sim}{K}$ influences the Doppler frequency. In addition, it is equally obvious that any component of velocity can be measured by properly orienting the difference vector $\underset{\sim}{K}$ by

changing the geometry of the incident and scattered light. In the remainder of this paper we shall adopt the convention that $\underset{\sim}{K}$ is aligned with the x-direction.

1.2 The Elementary Laser Doppler Anemometer

Because the frequency difference ω_D is added to or subtracted from the frequency of light it can be detected only by the mixing of radiation on a square law detector (as a photocell). There are many ways in which this can be done. They can be loosely grouped into reference beam and dual scatter systems.

In a reference beam system the scattered light is heterodyned on the photocell with unscattered or forward scattered reference radiation. A possible means by which this can be accomplished is the so-called Goldstein arrangement illustrated in figure 2.

If $E_s e^{i(\omega + \omega_D)}$ is the amplitude of the scattered light at the photocell and $E_r e^{i\omega t}$ is the amplitude of the reference radiation, the photocell output is given by

$$\text{output} \propto E_s^2 + E_r^2 + 2E_s E_r \cos \omega_D t \qquad 1.2.1$$

This last term contains the Doppler frequency which is linearly dependent on the velocity. This term will be called the Doppler current. One of the advantages of this system is that the amplitude of the Doppler current can be increased by increasing the strength of the reference beam.

The dual scatter system is illustrated in figure 3. In this arrangement, two beams are scattered through opposite angles and superimposed on the detector. If $E_{s1} e^{i(\omega + \frac{1}{2}\omega_D)t}$ and $E_{s2} e^{i(\omega - \frac{1}{2}\omega_D)t}$ represent the amplitudes of the scattered light at the detector, the output current is given by

$$\text{output} \propto E_{s1}^2 + E_{s2}^2 + 2E_1E_2 \cos \omega_D t \qquad 1.2.2$$

As before the last term is called the Doppler current.

The dual scatter system is often referred to as a fringe system since the two beam produce interference fringes when the flow is at rest. The Doppler frequency can be shown to be proportional to the rate at which fringes are crossed by the scattering center. The important parameter is then the fringe spacing which can easily be shown to be given by

$$d = \frac{\lambda_i}{2 \sin \theta/2} \qquad 1.2.3$$

From this last interpretation one of the advantages of the dual scatter system is obvious; namely that the Doppler frequency is independent of where the signal is observed.

Both of the above systems by themselves are unable to distinguish whether the velocity is positive or negative since it is impossible to measure the sign of the frequency. Directional sensitivity can be introduced by providing a fixed frequency shift to one of the beams. This is commonly accomplished by a Bragg tank or a rotating diffraction grating.

1.3 The Current Produced by a Single Scatterer

The incident and scattered radiation is not uniform in space but is limited by the finite width of the laser beams. Moreover the light scattered by all particles present is collected by the photocell; the output current is determined by the square of the vector sum of all the scattered light. Thus in addition to the term arising from the light scattered from a single particle, there are many more terms resulting from the cross products of light scattered from two particles.

Usually the phase changes across the scattering region cause the contribution of the cross terms to the total current to be negligible. This is referred to as incoherent scattering. Some investigators have successfully used systems in which the cross terms dominated; that is, coherent systems. The advantages of coherent systems are obvious; the signal amplitude is proportional to the number of scatterers present whereas for the incoherent case it is proportional to the square root of the number of particles present.

In this paper we shall assume that the LDA is operating with incoherent scattering. The modifications for the coherent case are straightforward. The important result for incoherent scattering is that the total signal current is the sum of the currents generated by the individual particles. Thus if i(t) is the total current

$$i(t) = \sum_{n=1}^{N(t)} i_{sp}^{(n)}(t) \qquad 1.3.1$$

where N(t) is the instantaneous number of contributing scatters and $i_{sp}^{(n)}(t)$ is the signal generated by the n^{th} scatterer.

The signal generated by a single particle can be written as

$$i_{sp}(t) = I(\underset{\sim}{x}) \cos \underset{\sim}{K} \cdot \underset{\sim}{x} \qquad 1.3.2$$

where $\underset{\sim}{x}$ is the particle position and $I(\underset{\sim}{x})$ is the space dependent amplitude. The particle position is given by

$$\underset{\sim}{x} = \underset{\sim}{a} + \int_o^t \underset{\sim}{U}(\underset{\sim}{a}, t_1)\, dt_1 \qquad 1.3.3$$

where $\underset{\sim}{a}$ is its initial position and $\underset{\sim}{U}(\underset{\sim}{a},t)$ is its velocity. $\underset{\sim}{a}$ serves to identify the particle since no two particles can be at the same location initially. Using this the particle current is then given by

$$i_{sp}(t) = I(\underset{\sim}{x}) \cos\left[\Omega + \underset{\sim}{K} \cdot \int_o^t \underset{\sim}{U}(\underset{\sim}{a},t_1)\, dt_1\right] \qquad 1.3.4$$

where Ω is a fixed phase depending on initial position

$$\Omega = \underset{\sim}{K} \cdot \underset{\sim}{a} \qquad 1.3.5$$

The velocity information we seek can be obtained by differentiating the phase

$$\frac{d}{dt}(\text{phase}) = \underset{\sim}{K} \cdot \underset{\sim}{U}(\underset{\sim}{a},t) = \omega_D \qquad 1.3.6$$

There are several things to note about this expression:

(i) The velocity obtained is a particle velocity. It may or may not correspond to the fluid velocity at the point.

(ii) Since the particle is moving the amplitude function $I(\underset{\sim}{x})$ is also varying with time, and can influence the determination of $\underset{\sim}{U}$.

(iii) It is valid only for a single particle.

1.4 Summary

The basic LDA has been introduced and an output proportional to velocity has been shown to be possible for a single particle. In the remainder of this paper the particles will be assumed to follow the flow, optical systems will be assumed perfect, and electronic devices will be assumed to possess the required slewing rates and frequency response to perform the required operations. This constitutes the ideal LDA.

Part I The Individual Realization LDA

2.1 Introduction

Individual realization anemometers by definition do not provide a continuous record of the velocity in the sampling volume. Moreover, since the particles arrive randomly, the data obtained is randomly collected. This, in itself, creates no serious problems. However, the number of particles which arrive having a particular velocity is, in general, dependent on the velocity. As a consequence, even if the particle distribution in space is statistically independent of the velocity field, the rate of particle arrival at the scattering volume can be dependent on the velocity field. This was first pointed out by McGlaughlin and Tiederman (1973)[16]. This phenomenon has serious implications on the types of averaging that can be used.

The problem can be illustrated by a simple example. Consider a step discontinuity in velocity (see figure 4). Assume the particles are statistically uniformly distributed in space; that is, the expected number of particles per unit volume at any instant is the same at any location. If we choose to observe the scattering volume at random instants in time, there is an equal probability that particle will be in either side of the scattering volume. Thus at any instant we have an equal probability of observing either a fast or a slow particle. This is a direct consequence of the assumption of spatial uniformity of the particle seeding.

On the other hand, suppose we observe continuously in time every particle which is swept through the volume. Since the volume flow rate through the fast part of the volume is greater, more fast particles will be observed. Clearly proper averages cannot be obtained by simply summing all the observations.

In general, one can say that more particles arrive during fast portions of the flow than during slow portions. This is even true if we take the limit as the sampling volume shrinks to zero, since the rate of particle arrival is influenced by its velocity. It is important to note that this does not mean that there are more fast particles than slow ones since that depends on the spatial extent of the "fast" or "slow" regions. This effect is not unique to LDA. A hot wire in a turbulent flow will also see more fluid particles moving with velocities above the mean than below. Nevertheless, it will yield a proper time average because the fast particles do not remain in the wire vicinity as long as do the slow ones. It is this observation which provides the key to proper statistical analysis of the individual realization LDA signals.

In the following sections we will analyze the velocity signal that is available for processing when no more than one particle is in the volume at a time. The analysis will assume that no data is accepted when more than one particle is present. The reason for this is that random phase fluctuations will be introduced by the presence of multiple particles which will lead to incorrect measured values. (Most commercial counters have a technique for eliminating samples taken when multiple particles are resident).

2.2 A statistical model

The scattering particles will be assumed to be statistically uniformly distributed in space; that is, the expected number of particles per unit volume is independent of location. This is possible only if the flow is incompressible and the flow is uniformly seeded. We will relax the incompressibility assumption later. In sections 2.2-2.4, the overbar will denote an ensemble average. The relation of this to time averages will be discussed in section 2.5.

The output from an instrument which yields a velocity while particles are in the scattering volume can be written as

$$\underset{\sim}{u}_o(t) = \iiint_{\text{all space}} w(\underset{\sim}{x})\ \underset{\sim}{u}(\underset{\sim}{x},t)\ g_1(\underset{\sim}{x})\ d\underset{\sim}{x} \qquad 2.2.1$$

The volume integral is taken over all space but it is effectively truncated by the function $w(\underset{\sim}{x})$ which specifies the shape of the scattering volume.[+] (Note that the scattering volume $w(\underset{\sim}{x})$ used here corresponds to the part of the flow from which the anemometer receives signals). The scattering volume V is then given by

$$V \equiv \iiint_{\text{all space}} w(\underset{\sim}{x})\ d\underset{\sim}{x} \qquad 2.2.2$$

The function $g_1(\underset{\sim}{x})$ accounts for the presence or absence of a particle at location $\underset{\sim}{x}$. The subscript 1 reminds us that we are interested only in situations where one particle is in the volume. Consistent with our assumption that the particles are statistically uniformly distributed is the assumption that they are Poisson distributed in space. Thus the probability of finding n particles in the volume V is

$$P_V(n) = \frac{(\mu V)^n}{n!}\ e^{-(\mu V)} \qquad 2.2.3$$

where μ is the volume concentration of scattering particles and V is the volume. It follows immediately that the probability of finding zero or one particle in the volume V is

$$1 - \sum_{n=2}^{\infty} n\ P_V(n) = \mu V\ (1 - e^{-\mu V}) \equiv \mu_1 V \qquad 2.2.4$$

[+] The $w(\underset{\sim}{x})$ used here differs from that in George and Lumley (1973) by a factor of 1/V where V is given by equation 2.2.2.

We can immediately compute the moments of $g_1(\underset{\sim}{x})$ in a manner similar to that used in George and Lumley (1973).

$$\overline{g_1(\underset{\sim}{x})} = \mu_1 \qquad 2.2.5$$

$$\overline{g_1(\underset{\sim}{x})g_1(\underset{\sim}{x}')} = \mu_1 \delta(\underset{\sim}{x}-\underset{\sim}{x}') \qquad 2.2.6$$

2.3 Mean Velocity

Since the occurrence of a particle at $\underset{\sim}{x}$ is independent of the velocity field we can compute

$$\overline{u_o(t)} = \mu_1 V \left[\frac{1}{V} \iiint w(\underset{\sim}{x}) \, \overline{u(\underset{\sim}{x},t)} \, d\underset{\sim}{x} \right] \qquad 2.3.1$$

The weighted integral of $u(\underset{\sim}{x})$ means that the velocity we get is averaged over the scattering volume. If the scattering volume is symmetric, then the volume averaged mean velocity

$$\overline{u_V} = \frac{1}{V} \iiint w(\underset{\sim}{x}) \, \overline{u(\underset{\sim}{x})} \, d\underset{\sim}{x} \qquad 2.3.2$$

differs from the average velocity at the center of the volume only if the mean velocity profile has curvature. This was first observed by Edwards et al (1970).

The factor $\mu_1 V$ is due to the fact that the velocity measured is not a continuous signal but rather a random sampling of the true velocity. By eliminating realizations where multiple particles are present, we have insured that $\mu_1 V \leq 1$. This is illustrated in figure (5). The length of the samples segments is purposely distorted since the slow moving particles will in general take longer to traverse the volume in a given direction than will the faster particles. This will be discussed later. In effect, if averages are performed by time averaging, the $\mu_1 V$ factor reduces the true average to account for the frac-

tion of time the output velocity is zero. This is easily seen from the following equation which substitutes the normal time average for the ensemble average.

$$\overline{u_V} = \lim_{T \to \infty} \frac{1}{T} \int_o^T u_V \, dt = \lim_{T \to \infty} \frac{1}{\mu_1 VT} \int_o^T u_o \, dt \qquad 2.3.3$$

2.4 Mean Square Velocity and the Autocorrelation

The autocorrelation of the effective velocity signal is given by

$$\overline{u_o(t)u_o(t')} = \iint w(\underset{\sim}{x})w(\underset{\sim}{x}') \; \overline{u(\underset{\sim}{x},t)u(\underset{\sim}{x}',t')} \; \overline{g_1(\underset{\sim}{x})g_1(\underset{\sim}{x}')} \; d\underset{\sim}{x}d\underset{\sim}{x}$$

$$= \mu_1 V \left[\frac{1}{V} \int w^2(x) \; \overline{u(\underset{\sim}{x},t)u(\underset{\sim}{x},t')} \; d\underset{\sim}{x} \right] \qquad 2.4.1$$

Separating mean and fluctuating velocities by

$$u = \overline{U} + u' \qquad 2.4.2$$

we obtain

$$\overline{u_o(t)u_o(t')} = \mu_1 V \left[\frac{1}{V} \int w^2(\underset{\sim}{x}) \; \overline{U}^2(\underset{\sim}{x}) \; dx \right]$$

$$+ \mu_1 V \left[\frac{1}{V} \int w^2(\underset{\sim}{x}) \; \overline{u'^2(\underset{\sim}{x})} \; \rho(\tau) \; d\underset{\sim}{x} \right] \qquad 2.4.3$$

where the mean flow has been assumed steady, the fluctuating velocities stationary and $\overline{u'(t)u'(t')} = \overline{u'^2}\rho(\tau)$ where $\tau = t' - t$.

The first term on the right hand side of Equation (2.4.3) is time independent and serves to subtract out the mean part of the cross correlation; the second term is just a volume averaged mean square fluctuating velocity which can be defined by

$$\overline{u_V'^2} = \frac{1}{V} \int w^2(\underset{\sim}{x}) \; \overline{u'^2}(x) \; d\underset{\sim}{x} \qquad 2.4.4$$

Using this equation (2.4.3) can be rewritten as

$$\overline{u_o(t)u_o(t+\tau)} = \mu_1 V\left[A + \overline{u_V'^2}\,\rho(\tau)\right] \qquad 2.4.5$$

where

$$A \equiv \frac{1}{V}\int w^2(\underset{\sim}{x})\,\overline{U}^2(\underset{\sim}{x})\,d\underset{\sim}{x} \qquad 2.4.6$$

Except for the constant zero offset A and the factor $\mu_1 V$ accounting for the dropout time, this is just the autocorrelation of the volume-averaged fluctuating velocity. Thus even though the signal is significantly disrupted by the random particle arrival and the dropout between particles, all of the <u>real time</u> information is retained intact.

It follows immediately that the mean square velocity is

$$\overline{u_o^2} = \mu_1 V\left[A + \overline{u_V'^2}\right] \qquad 2.4.7$$

and the power spectrum is

$$S_{u_o}(w) = \mu_1 V\left[A\delta(\omega) + S_{u_V}(\omega)\right] \qquad 2.4.8$$

where S_{u_V} is the volumed averaged spectrum defined by

$$\overline{u_V'^2} = \int S_{u_V}(\omega)\,d\omega$$

It is important to note that <u>although all real time information is retained, the techniques used to process the signal and the averaging times necessary may be significantly different from those customarily used because of the signal dropout</u>.

2.5 <u>Signal Processing of Single Particle Arrivals</u>

The ensemble averaging used to obtain the above results can be translated directly to time averaging if the flow is statistically stationary. In the

following paragraphs, the proper techniques for performing this averaging are discussed.

The averages we want all are of the same form; in particular, for the mean velocity we have

$$\bar{u}_o \cong \frac{1}{T}\int_o^T u_o \, dt = \frac{\mu_1 V}{T}\int_o^T u_V \, dt \qquad 2.5.1$$

or

$$\bar{u}_V \cong \frac{1}{\mu_1 VT}\int_o^T u_o \, dt \qquad 2.5.2$$

Thus we need not only to integrate u_o but we need to know $\mu_1 V$. However $\mu_1 VT$ is just the total time that there are particles in the volume. Therefore we can perform the average by integrating the effective velocity for a fixed time T and by keeping track of the length of time $\mu_1 VT$ for which there is a signal.

Most commercially available counters yield a single velocity realization for each particle arrival. The averages above can <u>not</u> be obtained by simply summing these realizations. Rather, each realization must be weighted by the length of time that the realization is representative of the velocity in the volume. In general, this length of time will depend on the particle velocity vector and the scattering volume geometry. For example, slow moving particles will be representative of the velocity in the scattering volume longer than will fast moving particles. To illustrate this, suppose the particles arrive at times t_1, t_2, ... and that they remain in the volume for times Δt_1, Δt_2, ... where the Δt's vary from particle to particle. Then from equation (2.5.2) we have

$$\bar{u}_V = \frac{1}{\sum_n \Delta t}\left\{\int_{t_1}^{t_1+\Delta t_1} u(t)dt + \int_{t_2}^{t_2+\Delta t_2} u(t)dt + \ldots\right\} \qquad 2.5.3$$

If we assume that the velocity is reasonably constant over times Δt, then the integral can be approimated by

$$\bar{u}_V \cong \frac{1}{\sum_{i=1}^{N} \Delta t_1} \left\{ \sum_{i=1}^{N} u(t_i) \cdot \Delta t_i \right\} \qquad 2.5.4$$

Similarly for the mean square velocity

$$\overline{u^2}_V = \frac{1}{\sum_{i=1}^{N} \Delta t_1} \sum_{i=1}^{N} u^2(t_i)\Delta t_i \qquad 2.5.5$$

If the scattering volume is spherical and of diameter d, then $\Delta t = \frac{d}{|u_i|}$ and the results of McGlaughlin and Tiederman for velocity bias are obtained. The exact relationship between the two techniques will be explored later.

It is clear from the preceding that unbiased velocity averages <u>are</u> available from individual realization anemometers. The signal processing, however, must keep track of the particle residence time.

2.6 <u>The Effect of Density Fluctuations</u>

If density fluctuations are significant, the assumption that the particles are statistically uniformly distributed in space may not be valid. In those situations, it may be possible if the particle seeding is uniform to assume that the distribution of particles <u>per unit mass</u> is uniform. The function $g'(\underset{\sim}{x})$ which accounts for the presence or absence of a particle at $\underset{\sim}{x}$ can be shown to have averages given by

$$\frac{\overline{g'(\underset{\sim}{x})} = \mu_2 \overline{\rho(\underset{\sim}{x})}}{g'(\underset{\sim}{x})g'(\underset{\sim}{x}') = \mu_2 \rho(\underset{\sim}{x})\, \delta(\underset{\sim}{x}-\underset{\sim}{x}')} \qquad 2.6.1$$

ed note: two equations

Since the g's depend on density which in turn can depend on the velocity field,

statistics of products of u and g must be computed together.

The effective velocity now becomes

$$u_o(t) = \iiint u(\underset{\sim}{x},t)w(\underset{\sim}{x})g'(\underset{\sim}{x})\, d\underset{\sim}{x} \qquad 2.6.2$$

and

$$\begin{aligned}\overline{u_o(t)} &= \iiint \overline{u(\underset{\sim}{x},t)g'(\underset{\sim}{x})}\, w(\underset{\sim}{x})d\underset{\sim}{x} \\ &= \mu_2 \iiint \overline{u(\underset{\sim}{x},t)\rho(\underset{\sim}{x})}\, w(\underset{\sim}{x})\, d\underset{\sim}{x} \\ &= \mu_2 \Big\{\iiint \overline{U(\underset{\sim}{x},t)}\ \overline{\rho(\underset{\sim}{x})}\ d\underset{\sim}{x} \\ &+ \mu_2 \iiint \overline{u'(\underset{\sim}{x})\rho(\underset{\sim}{x})}\ d\underset{\sim}{x}\Big\} \qquad 2.6.3\end{aligned}$$

The first term is significantly different from the previous result only if there are significant mean density gradients across the volume. The second term can be important only when the fluctuating velocity and density are well correlated and their relative intensities high.

In analogous fashion the mean square effective velocity can be obtained as

$$\begin{aligned}\overline{u_o^2(t)} &= \mu_2 \iiint \overline{u^2(\underset{\sim}{x},t)\rho(\underset{\sim}{x},t)}\, w^2(\underset{\sim}{x})\, d\underset{\sim}{x} \\ &= \mu_2 \iiint \overline{U^2(\underset{\sim}{x},t)}\ \overline{\rho(\underset{\sim}{x},t)}\, w^2(\underset{\sim}{x})\, d\underset{\sim}{x} \\ &+ \mu_2 \iiint \overline{u'^2(\underset{\sim}{x},t)\rho(\underset{\sim}{x})}\, w^2(\underset{\sim}{x})\, d\underset{\sim}{x} \qquad 2.6.4\end{aligned}$$

It should be noted explicitly that these results should be expected to be valid only if their number of particles per unit mass does not depend on location in the flow. In other words, the flow must be uniformly seeded.

2.7 Relation to other work

The approach used here must be contrasted with the approach that has been suggested by McGlaughlin and Tiederman[16] who first called attention to the fact that the usual methods for averaging discrete realizations as a randomly sampled time series were not correct. For example, the mean velocity cannot be computed from

$$\bar{u} = \frac{1}{N} \sum_{i=1}^{N} u_i$$

McGlaughlin and Tiederman showed that correct flow averages could be obtained by writing averages in a probabilistic form where the probability of occurrence of a particular velocity is proportional to the concentration of particles having that velocity. Thus the particle averaged mean velocity is given by

$$\bar{u} = \frac{\Sigma\, c[u_i]u_i}{\Sigma\, c[u_i]}$$

The difficulty with this approach lies in the inability to evaluate $c[u_i]$ in all but the simple case of spherical scattering volume and uniform steady flow. The results derived in this paper can be taken to show that when the particles are uniformly distributed in space or mass, $c[u_i]$ = particle residence time. This means that the concentration of slow particles is in fact greater than the concentration of fast particles, a conclusion opposite to that of McGlaughlin and Tiederman. In spite of the difference, though, the correct result is the same. Note that this result does not depend on the shape of the scattering volume or the type of flow field, but on the particle distribution in space.

An alternate approach to the bias problem derives from the fact that if a time signal is sampled at statistically independent intervals in time, the spectrum of the sampled signal is the same as the signal itself (c.f. Lumley 1970)[14]. The randomly arriving scattering particles do not arrive at intervals independent of the velocity; hence, they do not satisfy the criterion above. Durao and Whitelaw[4] successfully overcame the bias introduced by this correlation between arrival time and velocity by sampling the already discrete samples at random instants in time by a Poisson sampling device. The disadvantage of this approach is the large amount of data that is not processed.

Owen and Rodgers[18] in another part of these proceedings, analyze the problems of discrete realization anemometry and continuous signal anemometry in essentially the same manner as that demonstrated here with similar results. In addition, they consider the particular situation when the dropped out or discretely arriving signal is treated as a continuous signal by holding the last value until a new particle arrives. As would be expected from the preceding analysis, the results can be grievously in error. It is important to note that their results are not applicable to the continuous signals treated later in this paper because dropout there is <u>not</u> due primarily to the absence of particles.

Buchhave[3], in another paper in this proceedings, examines the problem arising from the fact that particles entering the flow from certain directions generate no signal or not enough signal for processing. In effect, the volume cross section depends on the direction of particle motion. This can cause deviations from ideal performance. The effect can be minimized by using frequency shifting techniques to increase the number of fringes and thereby increase the probability of detection.

Asalor and Whitelaw[1] in another paper in this volume have analyzed in detail the problems associated with density fluctuations and non-uniform seeding distributions. Their experimental results indicate that in many situations the assumptions of uniform seeding are valid.

Finally, the work of Mayo (1974)[15] must be mentioned because it addresses the problem of constructing the power spectrum from individual realizations of the velocity. Early versions of this work assumed that particle arrival and velocity were uncorrelated. In addition, each sample was treated identically in the analysis. While these changes are significant to the result in many flow situations, the work is significant in that it showed that such measurements can be made even with a badly disrupted signal. The work of Wang in this volume utilizes techniques similar to those of Mayo.

2.8 The application of various signal processing techniques to discrete realization velocimetry.

There are numerous devices available for converting the frequency-coded Doppler velocity information to voltage information. These may be loosely grouped into discrete and continuous signal processors. Either can be used for individual realization anemometry. In the following paragraphs the advantages and shortcomings of these devices as they relate to individual realization anemometry will be discussed.

Continuous signal processors provide an output during the entire time that the particle is in the volume. (The term scattering volume as used here includes the signal threshhold of the detector). This is of course the type of signal that is desired to perform the averages above. However, the output of the processor when no particle is present is crucial to proper use of the instrument. Most commercially available devices hold the last velocity until

the next particle arrives. This is not correct and can significantly bias the statistics if there are more fast particles than slow particles in which case the signal is more likely to drop out holding the fast value. Obviously the opposite can also be true if there were more slow than fast particles. Proper use of the instrument would require setting the signal equal to zero during the periods when no particles are present. Since it is necessary to keep track of the time that a particle is present, an additional output is necessary.

A second problem with most continuous signal processors is that they provide no means of eliminating those samples acquired when there is more than one particle present. (The reason for limiting the signal to single particle realizations will be clear after a discussion of the random phase fluctuations). This limitation is not serious if the concentration of particles is sufficiently low.

Discrete signal processors accept a given number of pulses of the signal and determine the period. This is, of course, a direct determination of the Doppler frequency and, hence, the velocity. Several techniques have been suggested which allow rejection of multiple particle realizations. It is important to note that the velocity determination alone is not sufficient to permit proper averaging; the length of time for which the sample is characteristic of the velocity in the sample volume must also be provided. This can be accomplished in several ways; for example, measuring the envelope width of the pulse produced by the burst or, by generating many counts from the same particle where the number of counts is proportional to the residence time. The paper by Hösel and Rodi [11] in this proceedings suggests a means by which the envelope width can be measured; the fast recycle time of the DISA counter, in effect, corrects for residence time if the one dimensional correction is applied.

Part II The Continuous LDA

3.1 The unsteady Doppler current with an arbitrary number of particles

With the restrictions detailed in the chapter 1, the Doppler current can be written as

$$i(t) = \frac{1}{N(t)} \int_{\text{all space}} i_{sp}(t,\underset{\sim}{a})\, g(\underset{\sim}{a})\, d\underset{\sim}{a} \qquad 3.1.1$$

where $i_{sp}(t,\underset{\sim}{a})$ is the time dependent current generated by the particle that was at $\underset{\sim}{a}$ at time $t = 0$, where $g(\underset{\sim}{a})$ accounts for the presence of or absence of the particle at $\underset{\sim}{a}$, and where $N(t)$ is the instantaneous number of particles in the volume. This expression is exactly equivalent to the sum

$$i(t) = \frac{1}{N(t)} \sum_{\substack{\text{particles} \\ \text{in the} \\ \text{volume}}} i_{sp}(t,n) \qquad 3.1.2$$

The current generated by a single particle is always of the form

$$i_{sp}(t,\underset{\sim}{a}) = I(\underset{\sim}{x}) \cos \underset{\sim}{K} \cdot \underset{\sim}{x} \qquad 3.1.3$$

where I is the envelope of the current (usually approximated as Gaussian), $\underset{\sim}{K}$ is the scattering wavenumber vector, and

$$\underset{\sim}{x} = \underset{\sim}{a} + \int_o^t \underset{\sim}{U}(\underset{\sim}{a},t_1)\, dt_1 \qquad 3.1.4$$

$\underset{\sim}{U}(\underset{\sim}{a},t)$ is the particle (Lagrangian by assumption) velocity.

It was shown by George and Lumley (1973)[7], p. 328 that this exact expression for the current could be reduced to

$$i(t) = [F^2 + G^2]^{\frac{1}{2}} \text{ as } [K X_o - \varphi]$$

where F and G are time dependent random variables and φ is a random phase defined by

$$\tan \varphi = \frac{G}{F} \qquad 3.1.6$$

X_o is an effective displacement given by

$$X_o = \int_o^t u_o(t_1)\, dt_1 \qquad 3.1.7$$

or

$$u_o(t) = \frac{dX_o}{dt} \qquad 3.1.8$$

where the effective velocity u_o is defined by

$$u_o(t) = \frac{1}{N(t)} \int_{\text{all space}} w[\underset{\sim}{x}(\underset{\sim}{a},t)]\; U(\underset{\sim}{a},t)\; g(\underset{\sim}{a})\; d\underset{\sim}{a} \qquad 3.1.9$$

For incompressible flow and for spacially homogeneous particle distributions this transforms to

$$u_o(t) = \frac{1}{N(t)} \int_{\text{all space}} w(\underset{\sim}{x})\; u(\underset{\sim}{x},t)\; g(\underset{\sim}{x})\; d\underset{\sim}{x} \qquad 3.1.10$$

The assumptions necessary for this transformation are usually valid for water experiments and for uniformly seeded low Mach number air experiments. It is convenient to define

$$g_n(\underset{\sim}{x}) = \frac{1}{N(t)}\; g(\underset{\sim}{x}) \qquad 3.1.11$$

Zero counting detectors, frequency and phase lack loops under ideal conditions yield an output which is proportional to the time derivative of the total phase of the input. From equation (3.1.5), the "velocity" output, u_d, from the anemometer is given by

$$u_d = u_o - \frac{1}{K}\, \dot{\varphi} \qquad 3.1.12$$

Thus our interpretation problem has two parts: (1) How does u_o correspond to the velocity we wish to measure; and (2) how do the fluctuations of $\dot{\varphi}$ influence the measurements? Both these questions will be addressed in the following paragraphs. In addition, some comments will be made about the characteristics of the current, $I(t)$, as they affect the ability of a detector to perform ideally.

3.1 The statistics of the effective velocity, $u_o(t)$

The mean effective velocity, $\overline{u_o(t)}$, is given by

$$\bar{u}_o = \int w(\underset{\sim}{x})\ \overline{u(\underset{\sim}{x},t)}\ \overline{g(\underset{\sim}{x})}\ d\underset{\sim}{x} = \frac{1}{V}\int w(\underset{\sim}{x})\ \overline{u(\underset{\sim}{x},t)}\ d\underset{\sim}{x} \qquad 3.2.1$$

since $g_n(\underset{\sim}{x}) = \frac{1}{V}$ and is uncorrelated with the velocity. (This follows immediately from the independence of $N(t)$ and $g(x)$ and the Appendix of George and Lumley 1973). As in section 2, the scattering volume is defined by

$$V = \int w(\underset{\sim}{x})\ d\underset{\sim}{x} \qquad 3.2.2$$

Hence u_o is just a volume averaged mean velocity and is the same as that velocity obtained for the individual realization case. If the profile has no curvature and the scattering volume is symmetric, the velocity accurately reflects the mean velocity at the center of the volume. (The factor μ, obtained in section 2.2 for the single particle case has been removed by averaging over the number of particles in the volume. In effect, this assumes that measurements are not accepted when there is no signal.

The autocorrelation of the effective velocity is given by

$$\overline{u_o(t)u_o(t')} = \iint_{\text{all space}} w(\underset{\sim}{x})w(\underset{\sim}{x}')\ \overline{u(\underset{\sim}{x},t)u(\underset{\sim}{x}',t')}\ \overline{g_n(\underset{\sim}{x})g_n(\underset{\sim}{x}')}\ d\underset{\sim}{x}d\underset{\sim}{x}' \qquad 3.2.3$$

It can be shown that if $N \gg 1$,

$$\overline{g_n(\underset{\sim}{x})g_n(\underset{\sim}{x}')} = \frac{1}{V^2} + \frac{1}{\bar{N}V}\ \delta(\underset{\sim}{x} - \underset{\sim}{x}') \qquad 3.2.4$$

where $\bar{N}$ is the expected number of particles in the volume.
It follows immediately that

$$\overline{u_o(t)u_o(t')} = \frac{1}{N}\frac{1}{V}\int w^2(\underset{\sim}{x})\ \overline{u(\underset{\sim}{x},t)u(\underset{\sim}{x},t')}\ d\underset{\sim}{x} + \frac{1}{V^2}\int w(\underset{\sim}{x})w(\underset{\sim}{x}')\ \overline{u(\underset{\sim}{x},t)u(\underset{\sim}{x}',t')}\ d\underset{\sim}{x}d\underset{\sim}{x}' \qquad 3.2.5$$

Separating the mean and fluctuating velocities and we have

$$\overline{u_o(t)u_o(t')} = \frac{1}{N}\left\{\frac{1}{V}\int w^2(x)\ U^2(\underset{\sim}{x})\ d\underset{\sim}{x} + \frac{1}{V}\int w^2(\underset{\sim}{x})\ \overline{u'^2(\underset{\sim}{x})}\ d\underset{\sim}{x}\right\} + \left\{\frac{1}{V}\int w(\underset{\sim}{x})\ U(\underset{\sim}{x})\ d\underset{\sim}{x}\right\}^2 + \frac{1}{V^2}\iint w(\underset{\sim}{x})w(\underset{\sim}{x}')\ \overline{u'(\underset{\sim}{x},t)u'(\underset{\sim}{x}',t')}\ d\underset{\sim}{x}d\underset{\sim}{x}' \qquad 3.2.6$$

Only the time dependent, fluctuating parts are of interest; that is,

$$\overline{u_o'(t)u_o'(t+\tau)} = \frac{1}{N}\left\{\frac{1}{V}\int w^2(\underset{\sim}{x})\ \overline{u'^2(\underset{\sim}{x})}\ d\underset{\sim}{x}\right\} + \frac{1}{V^2}\iint w(x)\ w(x')\ \overline{u'(x)u'(x',t')}\ dxdx' \qquad 3.2.7$$

Since we are interested here in continuous signals we can assume $\bar{N} \gg 1$ so that the correlation of interest is

$$\overline{u_o'(t)u_o'(t+\tau)} = \frac{1}{V^2}\iint w(\underset{\sim}{x})w(\underset{\sim}{x}')\ \overline{u'(\underset{\sim}{x},t)u'(\underset{\sim}{x}',t')}\ d\underset{\sim}{x}d\underset{\sim}{x}' \qquad 3.2.8$$

Thus the measured autocorrelation is a spatially filtered space time correlation of the velocity field.

The effect of this spatial averaging is most easily understood if we consider the case of homogeneous turbulence for which the three dimensional spectrum is given by

$$\text{F.T.}\ [\overline{u(\underset{\sim}{x})u(\underset{\sim}{x}+\underset{\sim}{r})}] = \Phi_{11}(k_1,k_2,k_3) \qquad 3.2.9$$

Defining the Fourier transform of $\frac{1}{V}\, w(\underset{\sim}{x})$ to be $W(\underset{\sim}{k})$ and Fourier transforming equation (3.2.8) we obtain

$$\overline{u_o'^2} = \iiint W(k)W^*(k)\ \Phi_{11}(k_1,k_2,k_3)\ dk_1dk_2dk_3 \qquad 3.2.10$$

The normally measured one dimensional spectrum $F_{11}^1(k_1)$ is defined by

$$\overline{u^2} = \int F_{11}^1(k_1)dk_1 \qquad 3.2.11$$

where

$$F_{11}^1(k_1) = \iint \Phi_{11}(\underset{\sim}{k})\ dk_2dk_3 \qquad 3.2.12$$

Because of the spatial averaging we obtain here

$$F_m(k_1) = \iint W(k)W^*(k)\ \Phi_{11}(k_1,k_2,k_3)\ dk_2dk_3 \qquad 3.2.13$$

where

$$\overline{u_o'^2} = \int F_m(k_1)\ dk_1 \qquad 3.2.14$$

Thus the transfer function of the measuring volume can be defined by

$$\frac{\text{measured spectrum}}{\text{true spectrum}} = \frac{F_m(k_1)}{F_{11}^1(k_1)} \qquad 3.2.15$$

Plots of this transfer function are shown in figure (6) for a Gaussian scattering volume of different sizes, relative to the Kolmogorov microscale. The attentuation at high wavenumbers is caused by the expected averaging of small scales across the measuring values. Figure (7) shows the spectra that might be measured for the scattering volumes used in figure (6). It is clear that scales smaller than the largest dimension of the scaterring volume cannot be measured. For further discussion of the spatial averaging the reader is referred to George and Lumley[7] (1973, p. 330).

4.1 The Statistics of the Doppler Current

We saw earlier that the instantaneous Doppler current could be written as

$$i(t) = [F^2 + G^2]^{\frac{1}{2}} \cos [K X_o - \varphi] \qquad 4.1.1$$

where

$$\tan \varphi = \frac{G}{F} \qquad 4.1.2$$

and

$$u_o = \frac{dX_o}{dt} \qquad 4.1.3$$

The statistics of u_o have been examined in the previous section and were seen, under appropriate restrictions, to parallel the statistics of the true velocity. We now turn to the statistics of the amplitude of the current, $[F^2 + G^2]^{\frac{1}{2}}$ and φ the phase fluctuations. The amplitude is important because it determines the detectability of the signal. The phase fluctuations are important because they add to the measured velocity to yield the detector output; that is,

$$u_d = u_o - \frac{1}{K} \dot{\varphi} \qquad 4.1.4$$

where u_d is the output "velocity".

George and Lumley[7] (1973, p. 338) were able to show that when the expected number of scattering particles in the volume is large ($N > 10$ is sufficient) i(t), F(t), and G(t) are Gaussian random variables. In addition, F and G are statistically independent. The Gaussian nature of F, G and i is important because of the many results for frequency modulated noise which have been developed over the last forty years. In the succeeding paragraphs, the application of these results to the continuous LDA will be detailed.

The random phase fluctuations (A simplified example)

It is instructive to begin by analyzing several idealized LDA situations.

Consider a uniformly illuminated, rectangular scattering volume with steady one dimensional flow (see fig. (8)a). Suppose there is only one scattering particle in the flow. Then the Doppler current is given by

$$\text{output} = \begin{cases} A \cos (Kut + \varphi); & \text{particle in volume} \\ 0 & \text{; particle in volume} \end{cases}$$

φ is determined by the time of entry. By determining the time between zero crossings, the particle velocity can be obtained.

Consider now the situation illustrated in fig. (8)b which differs from the previous example only in the fact that there are two particles in the volume which entered at different times. The output current is now given by:

$$\begin{aligned} i(t) &= A \cos (Kut + \varphi_1) + A \cos (Kut + \varphi_2) \\ &= 2A \cos (Kut + \varphi) \end{aligned}$$

where

$$\varphi = \tan^{-1} \left\{ \frac{\sin \varphi_1 + \sin \varphi_2}{\cos \varphi_1 + \cos \varphi_2} \right\}$$

while both particles are in the volume. When particle number 2 leaves the current abruptly changes to

$$i(t) = A \cos (Kut + \varphi_1)$$

Thus not only does the amplitude change, but the phase also changes abruptly. A typical signal for entering and leaving particles is illustrated in Fig. (8)c. Each of the abrupt phase changes causes anomalous zero crossings (either missing or extra crossings). A frequency determining device cannot distinguish these anomalous crossing from velocity fluctuations. It is also easy to see that as the particles enter and leave, the random phase associated with entry causes the signal to lose coherence. The coherence time is determined by the time it takes the entire population to change; that is, the transit time.

There are a number of other phenomena which can cause the signal to lose coherence. Consider the uniform shear flow situation depicted in fig. (8)d. If we choose two particles which entered at the same time, the output current is given by

$$i(t) = A \cos Ku_1 t + A \cos Ku_2 t$$

where u_1 and u_2 are the differeing velocities. It is easy to show by application of trigonometric identities that

$$i(t) = 2A \cos \left\{ K\left(\frac{u_1 - u_2}{2} \right) t \right\} \cos \left\{ K\left(\frac{u_1 + u_2}{2} \right) t \right\}$$

The second term is readily seen to have a frequency proportional to the mean velocity. The first term is an unsteady envelope which has a frequency proportional to velocity differences within the volume. This current is depicted in figure (8)d from which it is clear that an extra zero crossing is detected every time the envelope goes to zero. This is, of course interpreted as a velocity fluctuation. Naturally, there is an additional phase change when one particle leaves the volume.

Three interesting properties of the Doppler signal are evident in the preceding example: (1) velocity differences across the volume produce phase fluctuations, (2) these fluctuations are in addition to those caused by the changing particle population and (3) the Doppler envelope can go to zero, even when there are particles present. The phase fluctuations will be counted as velocity fluctuations unless a technique for discriminating against them can be devised. The fact that the envelope goes to zero can cause a serious problem for some continuous detection schemes using lock-in amplifiers.

In the real case, the phase changes are seldom as abrupt as those depicted in the preceeding examples. There are two reasons for this: (1) there are

many particles present, and (2) the scattering volume is usually a smooth, continuous function - instead of abrupt as in the example. As a result the phase changes continuously as the particles traverse the volume. In many situations the spectral distribution of the phase fluctuations overlaps that of the velocity; thus it is impossible to discriminate against them.

4.3 The Spectrum of the Doppler current

In the preceding examples we have seen that the current loses coherence because of the population change and because of the presence of velocity gradients in the scattering volume when more than one particle is present. George and Lumley[7] (1973, p. 327) have shown that for the usual situation where the scattering volume has a Gaussian cross section and where the turbulent displacements can be considered Gaussian, the autocorrelation of the Doppler current is given by

$$\overline{i(t)i(t+\tau)} = \tfrac{1}{2}\,\overline{i^2}\, e^{-(\Delta\omega)^2\tau^2/2} \cdot \left\{\overline{\cos K[X_o(t+\tau) - X_o(t)]}\right\} \qquad 4.3.1$$

where $\Delta\omega$ has been called the Doppler ambiguity bandwidth. (The choice of the word ambiguity arises from the ambiguities in velocity determination caused by the random phase fluctuations). Clearly the larger $\Delta\omega$ is, the more rapidly the signal loses coherence.

The ambiguity bandwidth can be related to the population turnover time and the velocity gradients by the following relationship

$$(\Delta\omega)^2 = (\Delta\omega)_L^2 + (\Delta\omega)_G^2 + (\Delta\omega)_T^2 + (\Delta\omega)_B^2 + (\Delta\omega)_R^2 + (\Delta\omega)_M^2 \qquad 4.3.2$$

where $\Delta\omega_L$ represents the effect of changing populating; $\Delta\omega_G$, the mean velocity gradient; $\Delta\omega_T$, the turbulent velocity gradients; $\Delta\omega_B$, the Brownian motion effects; $\Delta\omega_R$, refractive index fluctuations; and $\Delta\omega_M$, the non-monochromaticity of the laser source. Usually only the first three are important; these can

be shown to be related in the following manner to the flow properties;

$$\Delta\omega_L \propto \frac{1}{\text{transit time}} = \frac{\text{mean velocity}}{\text{scattering volume dimension}}$$

$$\Delta\omega_G \propto K\left|\vee \underset{\sim}{u}\right| \cdot \text{(scattering volume dimensions)}$$

$$\Delta\omega_T \propto K \text{ (rms velocity gradients)} \cdot \text{(scattering volume dimensions)}$$

(The exact relationships are not given here because of the dependence on scattering volume definitions. They can be easily obtained from George and Lumley 1973[7] or Berman and Dunning 1973[2]). Because $\Delta\omega_G$ and $\Delta\omega_T$ depend linearly on the size of the scattering volume while $\Delta\omega_L$ depends inversely on size, it is clear that for any given flow situation there is a choice of scattering volume which minimizes the ambiguity bandwidth $\Delta\omega$.

The term $\overline{\cos K\left[X_o(t+\tau) - X_o(\tau)\right]}$ in equation 4.3.1 is given to an excellent approximation by $\cos \omega_o \tau$ where ω_o is the instantaneous Doppler frequency corresponding to $\omega_o = Ku_o$. If $P(\omega_o)$ is the probability density of the Doppler frequency (in effect, the velocity probability density), then

$$\overline{i(t)i(t+\tau)} = \tfrac{1}{2}\,\overline{i^2}\, e^{-(\Delta\omega)^2\tau^2/2} \int_{-\infty}^{\infty} P_{\omega_o}(\omega_o) \cos \omega_o \tau \, d\omega_o$$

It follows immediately that the spectrum of the Doppler current is given by

$$I(\omega) = \int_{-\infty}^{\infty} I_A(\omega_1)\, p_{\omega_o}(\omega_1 - \omega)\, d\omega_1 \qquad 4.3.3$$

where I_A represents the effect of the ambiguity and is given by

$$I_A(\omega) = \frac{\overline{i^2}}{\sqrt{2\pi\Delta\omega}} e^{-\omega^2/2(\Delta\omega)^2} \qquad 4.3.4$$

and p_{ω_o} is the proability density of the frequency fluctuations caused by the turbulence since $\omega_o = K u_o$ it is proportional to the probability density of the volume averaged velocity.

The current spectrum in steady, uniform flow is readily obtained by substituting the appropriate probability density; that is

$$P_{u_o}(\omega) = \tfrac{1}{2}\delta(\omega - \bar{\omega}_o) + \tfrac{1}{2}\delta(\omega + \bar{\omega}_o) \qquad 4.3.5$$

since the velocity is steady. It follows that

$$\begin{aligned} I_{steady}(\omega) &= \tfrac{1}{2}\left[I_A(\omega - \bar{\omega}_o) + I_A(\omega + \bar{\omega}_o)\right] \\ &= \frac{\overline{i^2}}{2\sqrt{2\pi\Delta\omega}}\left[e^{-(\omega-\omega_o)^2/2(\Delta\omega)^2} + e^{-(\omega+\omega_o)^2/2(\Delta\omega)^2}\right] \end{aligned} \qquad 4.3.6$$

Thus, as expected, even the current spectrum in steady uniform flow has a finite width due to the phase fluctuations. For this reason the effect of the random phase fluctuations is sometimes referred to as the Doppler broadening.

For turbulent flow it is usually assumed that the probability density of the turbulence is Gaussian. In such cases the current spectrum becomes

$$I(\omega) = \frac{\overline{i^2}}{\sqrt{2\pi\left[(\Delta\omega)^2 + K^2\overline{u_o'^2}\right]}} \left\{ e^{-(\omega-\bar{\omega}_o)^2/2\left[\overline{(Ku_o')^2} + (\Delta\omega)^2\right]} + e^{-(\omega-\bar{\omega}_o)^2/2\left[\overline{(Ku_o')^2} + (\Delta\omega)^2\right]} \right\} \qquad 4.3.7$$

This is illustrated in figure (9). The mean square turbulent velocity can be obtained by subtracting $\Delta\omega$ from the spectral width. Note that because of the turbulent and velocity gradient influences on $\Delta\omega$ it is not sufficient merely subtract the laminar broadening.

The spectrum above is a poor approximation in regions where the mean velocity gradient has appreciable shear since the turbulence probability density is usually highly skewed. Such a spectrum is shown in figure (10).

Only by assuming that the turbulent probability densities are Gaussian can the intensity be obtained by subtraction of spectral widths since the measured spectrum is a convolution of phase fluctuating broadening with the probability density of the turbulence. In spite of this, however, the statistical moments of the volume averaged velocity can be obtained by integration of the current spectrum. This can easily be shown

$$\frac{1}{\bar{i}^2}\int_o^\infty \omega^n I(\omega)\, d\omega = \frac{1}{\bar{i}^2}\int_{-\infty}^{\infty} p_{\omega_o}(\omega_1)\left[\int_o^\infty \omega^n I_A(\omega_1 - \omega)\, d\omega\right] d\omega_1 \qquad 4.3.8$$

But

$$\frac{1}{\bar{i}^2}\int_o^\infty \omega^n I_A(\omega_1 - \omega)\, d\omega = \frac{1}{\bar{i}^2}\int_o^\infty \omega^n \left(\frac{1}{\sqrt{2\pi}\Delta\omega}\right) e^{-(\omega-\omega_1)^2/2(\Delta\omega)^2}\, d\omega \qquad 4.3.9$$

For n = 1 the integral reduces to $\omega_1/\overline{2i_2^2}$ and

$$\frac{1}{\bar{i}^2}\int_o^\infty \omega\ I(\omega)\, d\omega = \tfrac{1}{2}\int_{-\infty}^{\infty} \omega_1 p_{\omega_o}(\omega_1)\, d\omega = \bar{\omega}_o \qquad 4.3.10$$

For n = 2, the integral in (4.3.9) yields $[\omega_1^2 + (\Delta\omega)^2]/\overline{2i^2}$ from which we obtain

$$\frac{1}{\overline{i^2}} \int_o^\infty \omega^2 \, I(\omega) \, d\omega = \overline{\omega_o}^2 + (\Delta\omega)^2 + \overline{\omega_o'^2}$$

$$= K^2 \, (\overline{u_o}^2 + \overline{u_o'^2}) + (\Delta\omega)^2 \qquad 4.3.11$$

Thus moments higher than the first are affected by the phase fluctuation broadening even if obtained by integrating under the entire spectrum. Correction is possible, however, if $\Delta\omega$ is known independently.

Summary

In summary, the spectrum of the Doppler current has been analyzed for the multiple particle case. The current spectrum is like the probability density of the volume averaged velocity, but differs from it because of the random phase fluctuations. These random phase fluctuations broaden the spectrum and limit attempts to measure higher order moments from the spectrum. There exists an optimum scattering volume for each flow situation which minimizes the Doppler bandwidth and the resulting effect on the measurements.

It is important to note that no assumptions regarding processing techniques have been used. The ambiguity phenomena are solely a consequence of the presence of multiple particles in the volume and the resultant phase fluctuations. It is clear from this analysis why individual realization anemometers must be able to discriminate against multiple particle samples if they are to provide an improvement on continuous processing techniques.

5.1 Statistics of the Current Amplitude

We have seen that the Doppler current can be written as

$$i(t) = (F^2 + G^2)^{\frac{1}{2}} \cos (KX_o - \varphi) \qquad 5.1.1$$

where F and G are identically distributed Gaussian random variables and

$$\overline{F(t)F(t+\tau)} = \overline{G(t)G(t+\tau)} = \bar{F}^2 e^{-(\Delta\omega)^2\tau^2/2} \qquad 5.1.2$$

This signal resembles closely the classical F.M. noise signal analyzed by Rice[19] and others; that is

$$i_{F.M.}(t) = R(t) \cos(\omega t - \varphi) \qquad 5.1.3$$

The only difference is that the signal analyzed by Rice[17] has a linearly increasing phase (ω = constant) whereas for the unsteady Doppler signal the phase is time dependent.

George and Lumley[7] (1973, p. 338) have shown that the statistics of X_o and R were statistically independent. Hence the results of the classical theory are directly applicable. Of particular interest here are the probability density for R(t) and its level crossings.

It is straightforward to show by transforming F and G to polar variables R(t), Θ(t) and integrating out the angular dependence that the probability density for R is given by

$$p(R) = \frac{R}{\sqrt{i^2}} \exp\left\{-\frac{R^2}{2i^2}\right\} \qquad 5.1.4$$

This is sketched in fig. (11)

The probability distribution can be obtained by integration as

$$P(R < R_1) = \int_o^{R_1} p(R)\, dR \qquad 5.1.5$$

or

$$P(R < R_1) = 1 - \exp\left\{-\frac{R_1^2}{2i^2}\right\} \qquad 5.1.6$$

This is sketched in fig. (12).

It is clear that if the frequency demodulation has a finite detection level below which detection is not possible, there is always a finite probability that dropout will occur. The amount of dropout is inversely related to the rms signal current. Clearly the way to remedy dropout is to increase the signal level either by increasing the scattering particle density or by increasing the optical efficiency of the LDA system. Since $\overline{i^2} \propto \bar{N}$ and multiple scattering effects can cause signal deterioration if $\bar{N}$ is too large, the latter solution is often the only alternative.

The expected number of times the envelope R(t) passes through the value R_1 with positive slope has been derived by Rice (1949)[19] as

$$N_{R_1} = \Delta\omega \cdot p(R_1) \qquad 5.1.7$$

where $\Delta\omega$ is the Doppler bandwidth arising from the phase fluctuations and $p(R)$ is the probability density for R. Of particular interest is the fact that N_{R_1} is directly proportional to $\Delta\omega$. Thus by making the level crossing measurement, $\Delta\omega$ can be exactly determined since $p(R)$ is known. The importance of knowing $\Delta\omega$ has already been seen when we discussed the power spectrum; $\Delta\omega$ will take on added significance when we discuss the statistics of the demodulated velocity signal.

5.2 The Random Phase Fluctuations and the Instantaneous Velocity

The input current to the detector is of the form

$$i(t) = (F^2 + G^2)^{\frac{1}{2}} \cos (K X_o - \varphi) \qquad 5.2.1$$

where F and G are statistically, independent, identically distributed Gaussian random variables. The phase angle φ is given by

$$\tan \varphi = \frac{G}{F} \qquad 5.2.2$$

The ideal demodulator provides an output which is the time derivative of the total phase; that is

$$\frac{d}{dt} (KX_o - \varphi) = K u_o - \frac{d\varphi}{dt} \qquad 5.2.3$$

Thus the "velocity" output, say u_d is given by

$$u_d(t) = u_o(t) - \frac{1}{K} \frac{d\varphi}{dt} \qquad 5.2.4$$

The statistics of $\dot{\varphi}$ and u_o are statistically independent since u_o, F, and G are statistically independent. Using this fact we can derive the following relationships:

(i) the autocorrelation of u_d is given by

$$\overline{u_d(t)u_d(t+\tau)} = \overline{u_o(t)u_o(t+\tau)} + \overline{\dot{\varphi}(t)\dot{\varphi}(t+\tau)} \qquad 5.2.5$$

(ii) the mean square value of u_d is

$$\overline{u_d^2} = \overline{u_o^2} + \overline{\dot{\varphi}^2} \qquad 5.2.6$$

(iii) the spectrum of u_d is given by

$$S_{u_d}(f) = S_{u_o}(f) + S_{\dot{\varphi}}(f) \qquad 5.2.7$$

(iv) the probability density of u_d is the convolution of the probability densities of u_o and $\dot{\varphi}/K$.

$$p_{u_d}(u) = \int_{-\infty}^{\infty} p_{(u_o)}(x-u)\, p_{(\dot{\varphi}/K)}(x)\, dx \qquad 5.2.8$$

It is clear that the statistics of $\dot{\varphi}$, the random phase fluctuations, are important for velocity measurements from instantaneous LDA's. Before proceeding to examine the statistics of $\dot{\varphi}$ we note the following:

(i) F and G are Gaussian random variables with autocorrelations given by

$$\overline{F(t)F(t+\tau)} = \overline{G(t)G(t+\tau)} = \overline{F^2}\, e^{-(\Delta\omega)^2\tau^2/2} \qquad 5.2.9$$

where $\Delta\omega$ is the Doppler ambiguity bandwidth or broadening.

(ii) $R = (F^2 + G^2)^{\frac{1}{2}}$ is <u>not</u> an Gaussian random variable.

(iii) φ is <u>not</u> a Gaussian random variable and, in fact, is not even stationary.

(iv) $\dot{\varphi}$ is <u>not</u> a Gaussian random variable; it is, however, stationary.

Misinterpretation of the statistics of the Doppler signal have most frequently arisen from a misunderstanding of these properties (c.f. George and Berman (1973)[8] for examples).

5.3 Probability Density for $\frac{d\varphi}{dt}$

Rice (1949)[19] has shown that the probability density for $\dot{\varphi}$ is given by

$$p_{\dot{\varphi}}(\dot{\varphi}) = \tfrac{1}{2}\left[1 + \frac{\dot{\varphi}^2}{(\Delta\omega)^2}\right]^{-3/2} \qquad 5.3.1$$

This is graphed in fig. (13). It is clear that for large $\dot{\varphi}$, this rolls off as $\dot{\varphi}^{-3/2}$. The mean square value of $\dot{\varphi}$ can be obtained as

$$\overline{\dot{\varphi}^2} = \int_{-\infty}^{\infty} \dot{\varphi}^2\, p_{\dot{\varphi}}(\dot{\varphi})\, d\dot{\varphi} = \infty \qquad 5.3.2$$

Since the mean square output from the anemometer is $\overline{u_o^2} + \overline{\dot{\varphi}^2}$ it is clear that such measurements by themselves are meaningless!

The rate at which the tails of the distribution roll off is dependent only on $\Delta\omega$. This is reflected in the expected value of the absolute rate of phase fluctuation, $\dot{\phi}$, which is given by

$$\left|\dot{\phi}\right| = \Delta\omega \qquad 5.3.3$$

Since the measured probability density is the convolution of the probability densities of phase fluctuations and the flow velocity, it is clear from the smoothing property of a convolution that a reasonable approximation to the true flow velocity probability density is obtained only if

$$K\,\Delta\omega < u_o' \qquad 5.3.4$$

where u_o' is the rms fluctuating velocity. Because of the large weighting in the tails, even when this criterion is met the measured density is not valid far from the center of the distribution.

5.4 Autocorrelation

Lawson and Uhlenbeck[13] (1950) show that the autocorrelation of the random phase fluctuations is given by

$$\overline{\dot{\phi}(t)\dot{\phi}(t+\tau)} = \tfrac{1}{2}\left(\frac{\ddot{\rho}}{\rho} - \frac{\dot{\rho}^2}{\rho}\right) \ell n\ (1 - \rho^2) \qquad 5.4.1$$

where ρ is the autocorrelation $\overline{F(t)F(t+\tau)} = \overline{F^2}\,\rho(t)$ and $\dot{\rho}$, $\ddot{\rho}$ are its derivatives with respect to τ.

George and Lumley[7] (1973, p. 338) have shown that $\rho(\tau)$ is nearly Gaussian; and

$$\rho(\tau) = e^{-(\Delta\omega)^2\tau^2/2} \qquad 5.4.2$$

from which it follows that

$$\overline{\dot{\phi}(t)\dot{\phi}(t+\tau)} = -\frac{(\Delta\omega)^2}{2}\ \ell n\ (1 - \rho^2) \qquad 5.4.3$$

As $\rho \to 0$

$$\overline{\varphi(t)\varphi(t+\tau)} \to 0 \qquad 5.4.4$$

and as $\rho \to 1$

$$\overline{\varphi(t)\varphi(t+\tau)} \to \infty \qquad 5.4.5$$

Thus the autocorrelation of the random phase fluctuations is singular at the origin and $\overline{\dot{\varphi}^2} = \infty$ as observed earlier. Equation (5.4.3) is plotted in figure (14).

Recalling that the autocorrelation of the anemometer output is given by

$$\overline{u_d(t)u_d(t+\tau)} = \overline{u_o(t)u_o(t+\tau)} + \overline{\dot{\varphi}(t)\dot{\varphi}(t+\tau)} \qquad 5.4.6$$

it is clear that autocorrelation measurements will be seriously in error for small τ, regardless of the particular velocity autocorrelation, Fig. (15) demonstrates this with two autocorrelations measured in grid turbulence. The finite value at the origin reflects the effect of low pass filtering.

5.5 The Spectrum of $\dot{\varphi}$

The power spectrum of $\dot{\varphi}$ can be obtained from equation (5.4.3) by expanding the logarithm as a series and transforming term by term (c.f., Rice (1949))[19]. The result is

$$\Phi_{\dot{\varphi}}(\omega) = \frac{1}{4\sqrt{\pi}} \Delta\omega \sum_{n=1}^{\infty} n^{-3/2} \exp\left\{-\frac{\omega^2}{4n(\Delta\omega)^2}\right\} \qquad 5.5.1$$

The limiting forms of this are:

(i) as $\omega \to \infty$, $P_{\dot{\varphi}}(\omega) = \frac{(\Delta\omega)^2}{2\omega}$ 5.5.2

(ii) for $\omega < \Delta\omega$, $P_{\dot{\varphi}}(\omega) \simeq P_{\dot{\varphi}}(o)$ 5.5.3

(iii) $P_{\dot{\varphi}}(o) = 0.368\,\Delta\omega$ 5.5.4

The spectrum is plotted in figures (16) and (17). Once again we see that $\Delta\omega$ is the only parameter.

Because of the slow roll-off at high frequencies ($P_{\dot{\varphi}} \sim \omega^{-1}$), the spectrum of the phase fluctuations will dominate the spectrum of the anemometer output at high frequencies because

$$S_{u_d}(\omega) = S_{u_o}(\omega) + S_{\dot{\varphi}}(\omega) \qquad 5.5.5$$

where

$$S_{\dot{\varphi}}(\omega) = \frac{1}{K^2} P_{\dot{\varphi}}(\omega) \qquad 5.5.6$$

This effect is demonstrated in figure (18) with spectral measurements in turbulent pipe flow.

For many flows the only frequencies of interest are those for which $\omega \ll \Delta\omega$. In those case the spectrum of the phase fluctuations is effectively white with a constant height equal to its value at the origin. Since this height is directly proportional to $\Delta\omega$, it can be minimized by minimizing the bandwidth of the phase fluctuations. Examples of how this can be done can be found in George (1972)[6] and George and Lumley (1973)[7].

5.6 The effect of low pass filtering

Since any real LDA has a finite bandwidth, $\overline{\dot{\varphi}^2}$ is not really infinite. In most cases, however the phase fluctuations make a non-negligible and sometimes dominant contribution to the mean square measured velocity. It is instructive therefore, to examine the effect of a low pass filter on the phase fluctuations. This was done by George (1974)[9] for a simple low pass filter (-6dB/oct.). The low passed spectrum is given by

$$P_{\dot{\varphi}LP}(\omega) = \frac{1}{4\sqrt{\pi}} \sum_{n=1}^{\infty} n^{-3/2} \frac{\exp\left[-\omega^2/4n(\Delta\omega)^2\right]}{1 + (\omega/\omega_L)^2} \qquad 5.6.1$$

where ω_L is the -3dB frequency of the filter.

This can be integrated to yield the mean square low passed phase fluctuations as

$$\overline{\dot{\varphi}^2_{LP}} = (\Delta\omega)\frac{\sqrt{\pi}}{4} \sum_{n=1}^{\infty} n^{-3/2} \omega_L \left[1 - \mathrm{erf}\left(\frac{\omega_L}{2n\Delta\omega}\right)\right] \exp\left[\omega_L^2 4/n(\Delta\omega)^2\right] \qquad 5.6.2$$

If $\omega_L < \Delta\omega$, this is approximately given by

$$\overline{\dot{\varphi}^2_{LP}} \simeq 0.368\,\pi\,\omega_L\,\Delta\omega \qquad 5.6.3$$

which is exactly the result that would be obtained for an equivalent white noise signal.

George (1974)[9] showed that by using several cutoff frequencies and extrapolating to $\omega_L = 0$, the true mean square velocity fluctuation could be obtained. This procedure is illustrated in figure (19).

5.7 Reynolds stress and Cross correlations

An important application of the LDA to turbulence measurement is the measurement of the correlation between two velocity components at the same point in the fluid; that is, the turbulent Reynolds stress. This is commonly performed by taking two measurements with a single instrument. For the first measurement the instrument is aligned to measure the vector sum of two velocity components and for the second the vector difference. Typically the instantaneous outputs from the two measurements are given by

$$e_1 = Au + Bv \qquad 5.7.1$$

$$e_2 = Au - Bv \qquad 5.7.2$$

where A and B are coefficients determined only by geometry. Squaring and averaging yields the desired correlation as

$$\overline{uv} = \frac{1}{4AB}\left\{\overline{e_1^2} - \overline{e_2^2}\right\} \qquad 5.7.3$$

Consider now the effect of the phase fluctuations. The real outputs are given by

$$e_1 = Au + Bv + \varphi_1 \qquad 5.7.4$$

$$e_2 = Au + Bv + \varphi_2 \qquad 5.7.5$$

Squaring and averaging now yields the correlation as

$$\overline{uv} = \frac{1}{4AB}\left\{\overline{e_1^2} - \overline{e_2^2} + \overline{\varphi_1^2} - \overline{\varphi_2^2}\right\}$$

or

$$\overline{uv}\Big|_{\text{measured}} = \overline{uv}\Big|_{\text{true}} + \frac{\overline{\varphi_1^2} - \overline{\varphi_2^2}}{4AB}$$

Since the entire apparatus has been rotated between measurements, it is unlikely that $\overline{\varphi_1^2}$ and $\overline{\varphi_2^2}$ are exactly equal. Since both are usually large quantities, errors can be significant.

An alternate approach to the mesurement of Reynolds stress is to use two LDA's and simultaneously measure both u and v and their correlation. If the scattering volumes do <u>not</u> overlap, the phase fluctuations are uncorrelated and the measurements of the Reynolds stress is unaffected by the phase fluctuations. This was proven by George and Lumley (1973)[7] and has been confirmed experimentally by Morton and Clarke (1971).[17] This would then seem to be the best way to measure Reynolds stress but care must be taken to insure that the scattering volumes are not too far apart. As a general guideline, they should be within

the Kolmogorov microscale of the turbulence.

Because the phase fluctuations are uncorrelated between non overlapping scattering volumes, the dual LDA technique can be used to advantage in many applications. All two point correlations are, of course, possible and have been successfully measured. (See, for example, Morton and Clarke[17]). George (1971)[5] suggested that a possible way to eliminate the phase fluctuations in single point measurements was to use two LDA's measuring the same velocity component whose scattering volumes were within the Kolmogorov microscale. The cross spectrum in this case would be the usual velocity spectrum without the phase fluctuations. Van Maanen[20] in a paper included in these proceedings successfully applied this technique by utilizing a novel dual optical system.

In summary, the LDA would appear to be uniquely suited for cross spectral and cross correlation measurements of all types. The random phase fluctuations are not a problem to the careful experimentalist and the usual problem of probe interference is, of course, non existent. Joint probability distribution measurements will remain, however, subject to the same limitations as the single point measurements; the effect of the phase fluctuations will be to reduce the correlation between variables.

5.8 Summary and Conclusions

The effect of the random phase fluctuations on the instantaneous output of an LDA has been examined. All single point statistical quantities were seen to be influenced by the random phase fluctuations. In every case this effect can be exactly calculated if the Doppler bandwidth $\Delta\omega$ is known. Fortunately $\Delta\omega$ can be determined exactly by the level crossings of the current amplitude. Uncontaminated cross-sepctral and cross correlation measurements are possible if scattering volumes do not overlap.

The effect of additive electronic noise on the phase fluctuations has not been discussed here. George (1971)[5] has shown that the signal produced by a Doppler current and noise can be regarded as the sum of two bandpassed noise signals. Greated and Durrani (1971)[10] have applied this type of analysis to LDA signals.

The degree to which commercially available instruments approximate the ideal signal treated here varies from device to device. Detailed analysis of frequency and phase locked loops is not straightforward. Hence evaluation of the instrument must be carried out by simulated Doppler signals. A simulator which accurately models the true Doppler signal has been developed by Lading and Edwards[12] and is discussed in a paper in these proceedings. Fig. (20) shows a comparison of the simulator input with the output from three different detectors. Note that in spite of the slight differences, all outputs contain the broad band noise which is responsible for the spikes. This is not due to the device, but is a direct manifestation of the random phase fluctuations which are inherent in the signal.

References

1. Asalor, J. O. and J. H. Whitelaw (1976), The influence of combustion induced particle concentration variations on laser-Doppler anemometry, Proceedings LDA-Symposium, Copenhagen 1975.

2. Berman, N. S. and J. Dunning (1973), Pipe flow measurements of turbulence and ambiguity using laser Doopler velocimetry, J. Fluid Mech., Vol. 61, p. 289.

3. Buchhave, P. (1976), Biasing errors in individual particle measurements with the LDA-counter signal processor, Proceedings LDA-Symposium, Copenhagen 1975.

4. Durao, D. F. G. and J. H. Whitelaw (1976), The influence of sampling procedure on the velocity bias in turbulent flows, Proceedings LDA-Symposium, Copenhagen 1975.

5. George, W. K. (1971), The laser Doppler velocimeter and its application to the measurement of turbulence, Ph.D. Thesis, Dept. of Mechanics, The Johns Hopkins University, Baltimore, Md.

6. George, W. K. (1972), Limitations on the measurement of unsteady flow velocities with a laser Doppler velocimeter, Fluid dynamic measurements in the industrial and medical environment, Leicester Univ. Press, England.

7. George, W. K. and J. L. Lumley (1973), The laser Doppler velocimeter and its application to the measurement of turbulence, Jour. Fluid Mech., Vol. 60, p. 321.

8. George, W. K. and N. S. Berman (1973), Doppler ambiguity in laser Doppler velocimeters, Appl. Phys. Lett., Vol. 23, p. 222.

9. George, W. K. (1974), The measurement of turbulence intensities using real-time laser-Doppler velocimetry. Jour. Fluid Mech., Vol. 66, pt. 1, pp. 11-16.

10. Greated, C. A. and T. S. Durrani (1971), Signal analysis for laser velocity measurements, Journal of Physic E: Sci. Instr., Vol. 4.

11. Hosel, W. and W. Rodi (1976), Errors occuring in LDA measurements with counter signal processing, Proceedings LDA Symposium, Copenhagen 1975.

12. Lading, L. and R. V. Edwards (1976), The effect of measurement volume on laser Doppler anemometer measurements as measured on simulated signals, Proceedings LDA-Symposium, Copenhagen 1975.

13. Lawson, J. L. and G. E. Uhlenbeck (1950), Threshhold Signals (Dover ed. 1965), New York.

14. Lumley, J. L. (1970), Stochastic Tools in Turbulence, Academic Press, N.Y.

15. Mayo, W. T. (1974), A discussion of limitations and extensions of power spectrum estimation with Burst-Counter LDA Systems, Proceedings of the Second International Workshop on Laser Velocimetry, Purdue Univ., Vol. I, 1974, pp. 90-101.

16. McGlaughlin, D. K. and Tiederman, W. G. (1973), Biasing correction for individual realization laser anemometer measurements in turbulent flows, Phys. of Fluids, Vol. 16, No. 12, pp. 2082-2088.

17. Morton, J. B. and W. H. Clark (1971), Measurements of two-point velocity correlations in a pipe flow using laser anemometers, Jour. Phys. E: Scientific Instr., Vol. 4.

18. Owen, J. M. and R. H. Rodgers (1976), The effect of particle distribution on biasing in a laser Doppler anemometer, Proceedings LDA Symposium, Copenhagen 1975.

19. Rice, S. O. (1948), Statistical properties of a sine wave plus random noise, Bell System Technical Journal, Vol. 27, pp. 109-157.

20. van Maanen, H. R. E. (1976), Reduction of ambiguity noise in laser-Doppler velocimetry by a cross correlation techniques, Proceedings LDA Symposium, Copenhagen 1975.

21. Wang, J. C. F. (1976), Measurement accuracy of flow velocity via digital-frequency-counter laser velocimeter processor, Proceedings LDA Symposium, Copenhagen 1975.

List of Figure Captions

Fig. 1 Light incident at angle $\theta/2$ measured from the perpendicular to the velocity vector is collected at $\theta/2$. The difference wavenumber, $\underset{\sim}{K} = \underset{\sim}{k}_i - \underset{\sim}{k}_s$ is parallel to the velocity in this case.

Fig. 2 Reference beam geometry

Fig. 3 Dual scatter or "fringe" geometry

Fig. 4 Particles are uniformly distributed in space (statistically). Because of higher velocity more particles are swept through upper part of volume per unit time.

Fig. 5 Typical velocity signal from individually arriving particles.

Fig. 6 Typical transfer function resulting from averaging of turbulent fluctuations across the volume. $\tilde{m} \propto$ (largest scattering volume dimension)$^{-1}$.

Fig. 7 Turbulent spectra normalized in Kolmogorov variables showing effect of transfer function (Fig. 6).

Fig. 8 a) Signal generated by passage of single particle in steady, uniform flow.

b) Signal generated by two particles which entered the flow at different times.

c) Typical signal that would be obtained from many particles.

d) Signal generated by two particles having different velocities.

Fig. 9 a) Spectrum of Doppler current generated by single particle or by many particles in steady uniform flow.

b) Spectrum of Doppler current in typical turbulent flow.

Fig. 10 Spectrum of Doppler current obtained near the wall in turbulent pipe flow (Ref. 2). Dotted line shows spectrum corrected for electronic noise.

Fig. 11 Probability density of the amplitude of the Doppler current. Equation (5.3.1).

Fig. 12 Probability distribution function for amplitude of Doppler current. Equation (5.3.2).

Fig. 13 Probability density of random phase fluctuations.

Fig. 14 Autocorrelation of random phase fluctuations.

Fig. 15 Typical autocorrelations measured in turbulent flow using an LDA. Finite value for $\tau = 0$ reflects effect of finite bandwidth of detector.

Fig. 16 Spectrum of random phase fluctuations.

Fig. 17 Spectrum of random phase fluctuations measured in uniform, steady flow (Ref. 2).

Fig. 18 "Velocity" spectra measured in turbulent pipe flow showing effect of phase fluctuations at high frequencies. (Ref. 2).

Fig. 19 Effect of low pass filtering on mean square "velocity" signal from LDA. True mean square is obtained by extrapolating to zero filter frequency.

Fig. 20 True turbulence signal and that measured by three different detectors. Primary differences are due to random phase fluctuations although it is clear that there are differences in the detectors. (Ref. 12).

fig 1

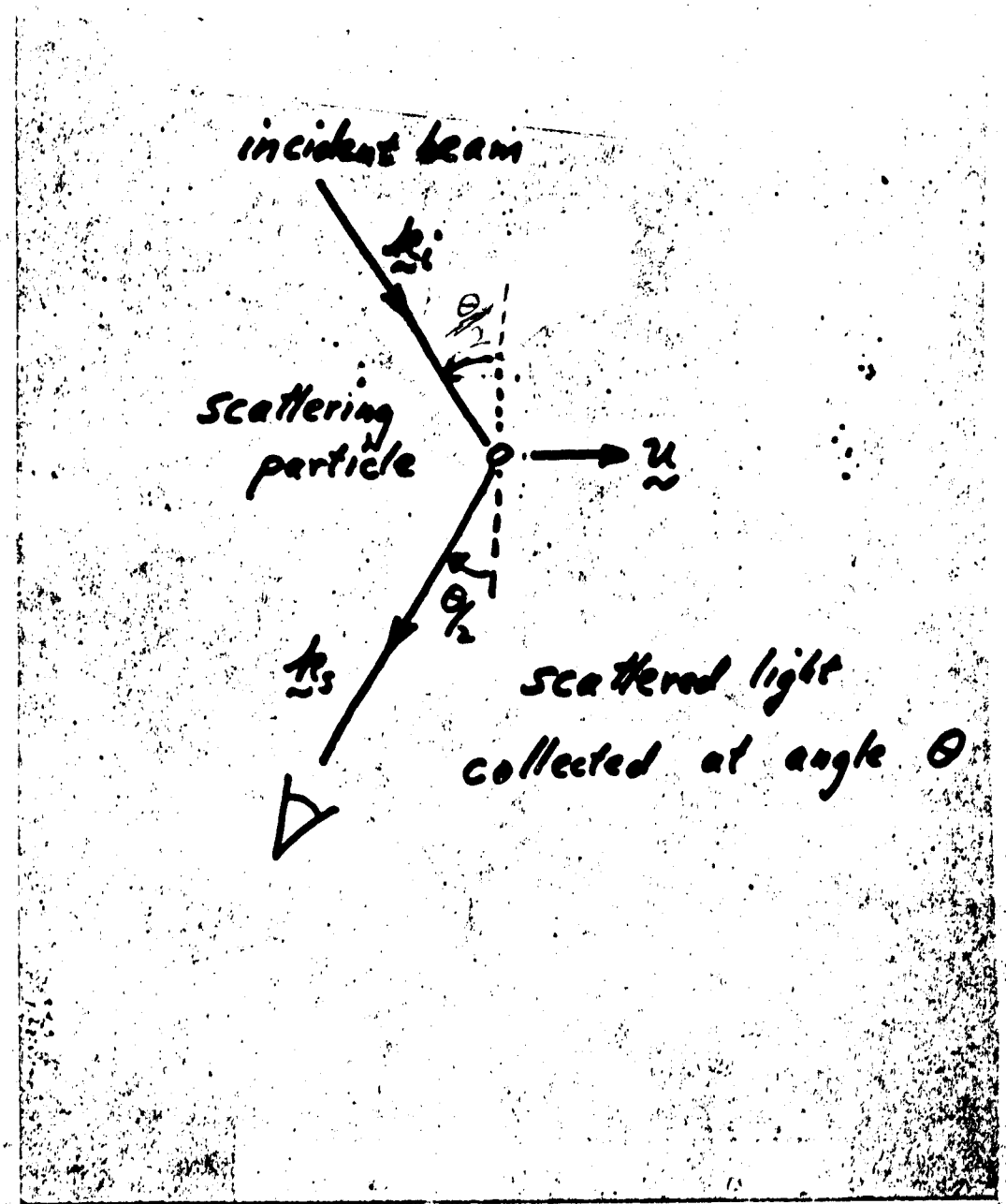
incident beam
k_i
$\theta/2$
scattering particle
O
u
$\theta/2$
k_s
scattered light
collected at angle θ

fig 2

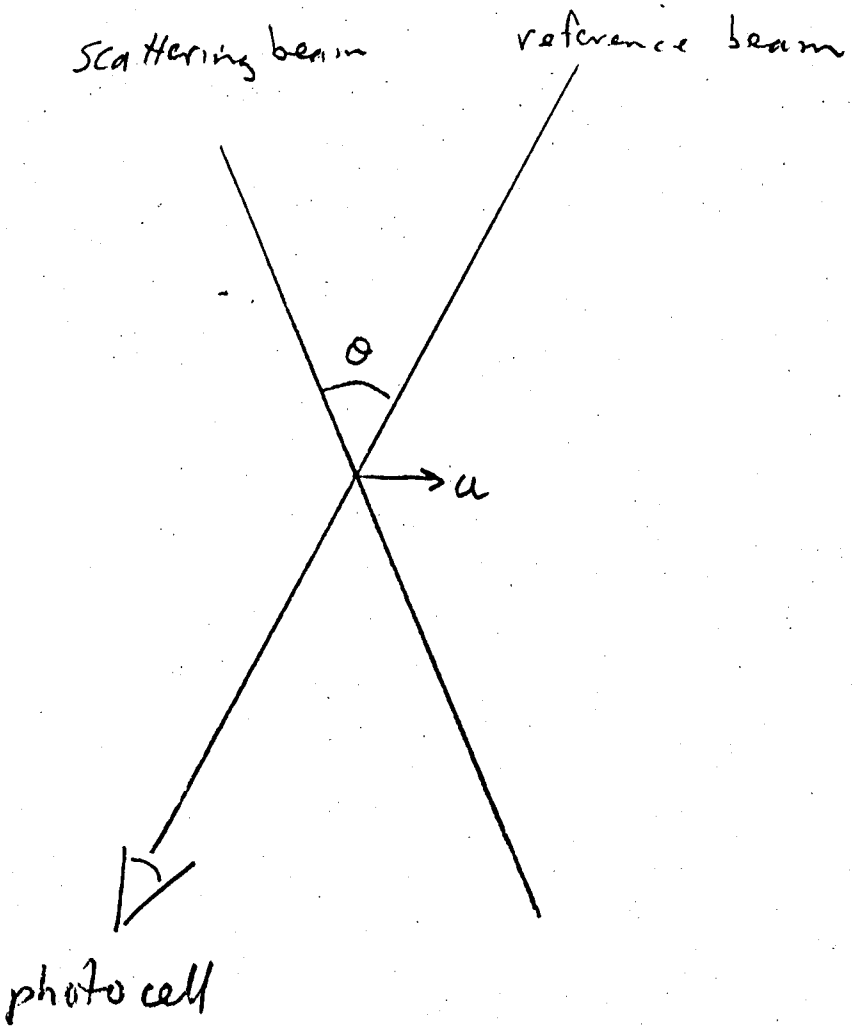

fig 3

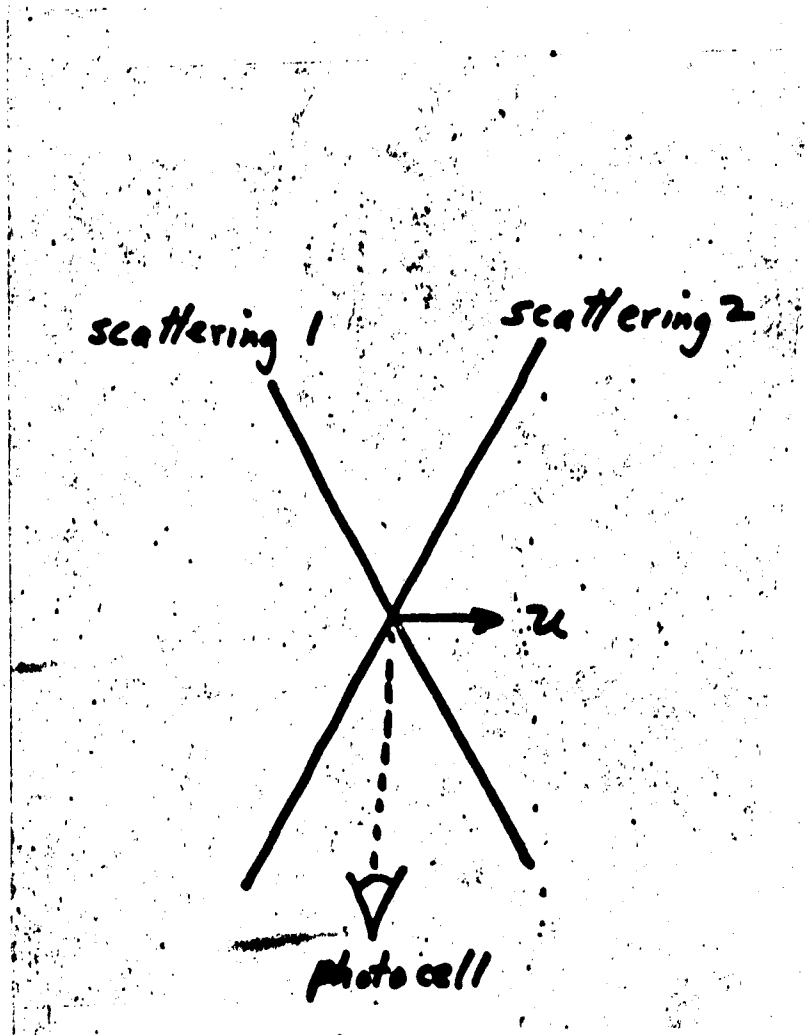

fig 1

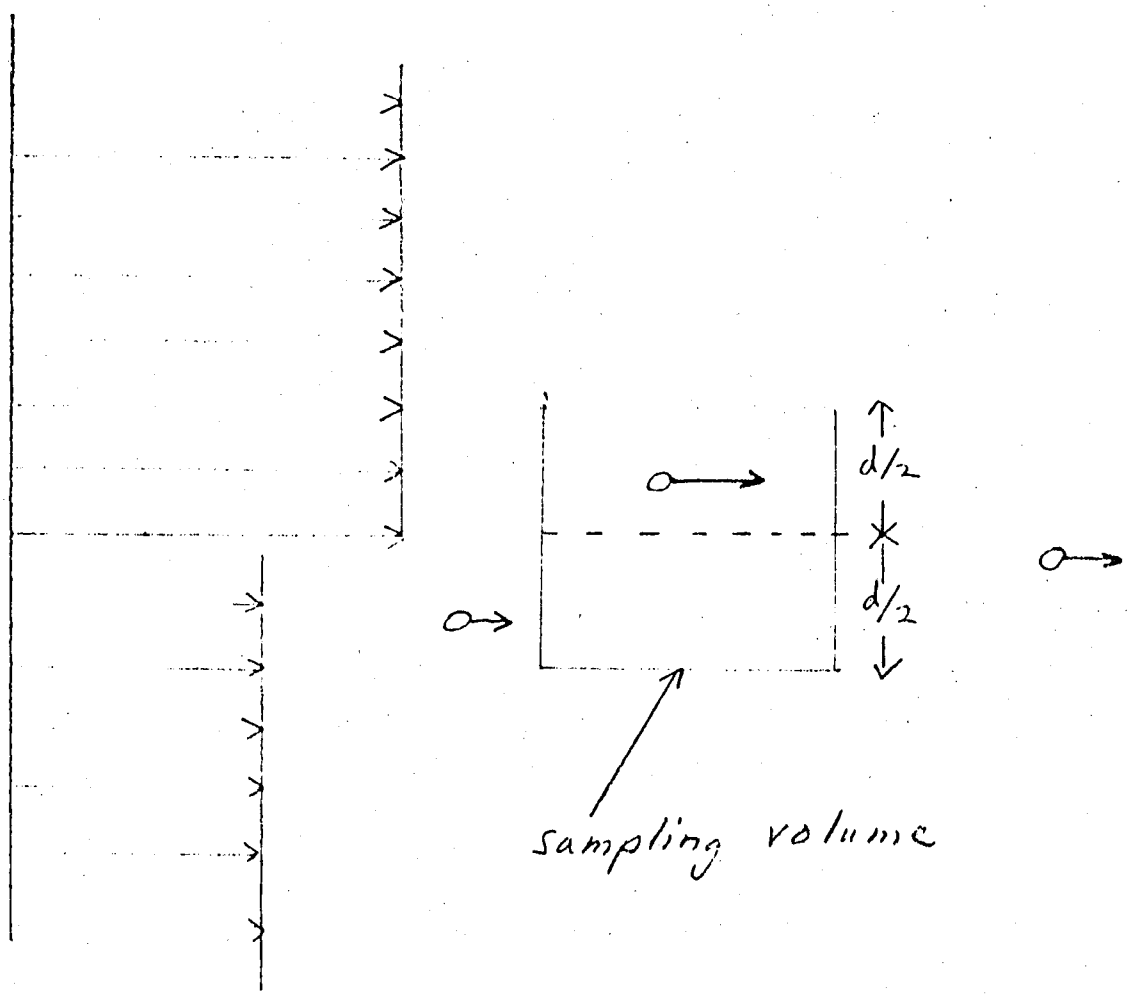

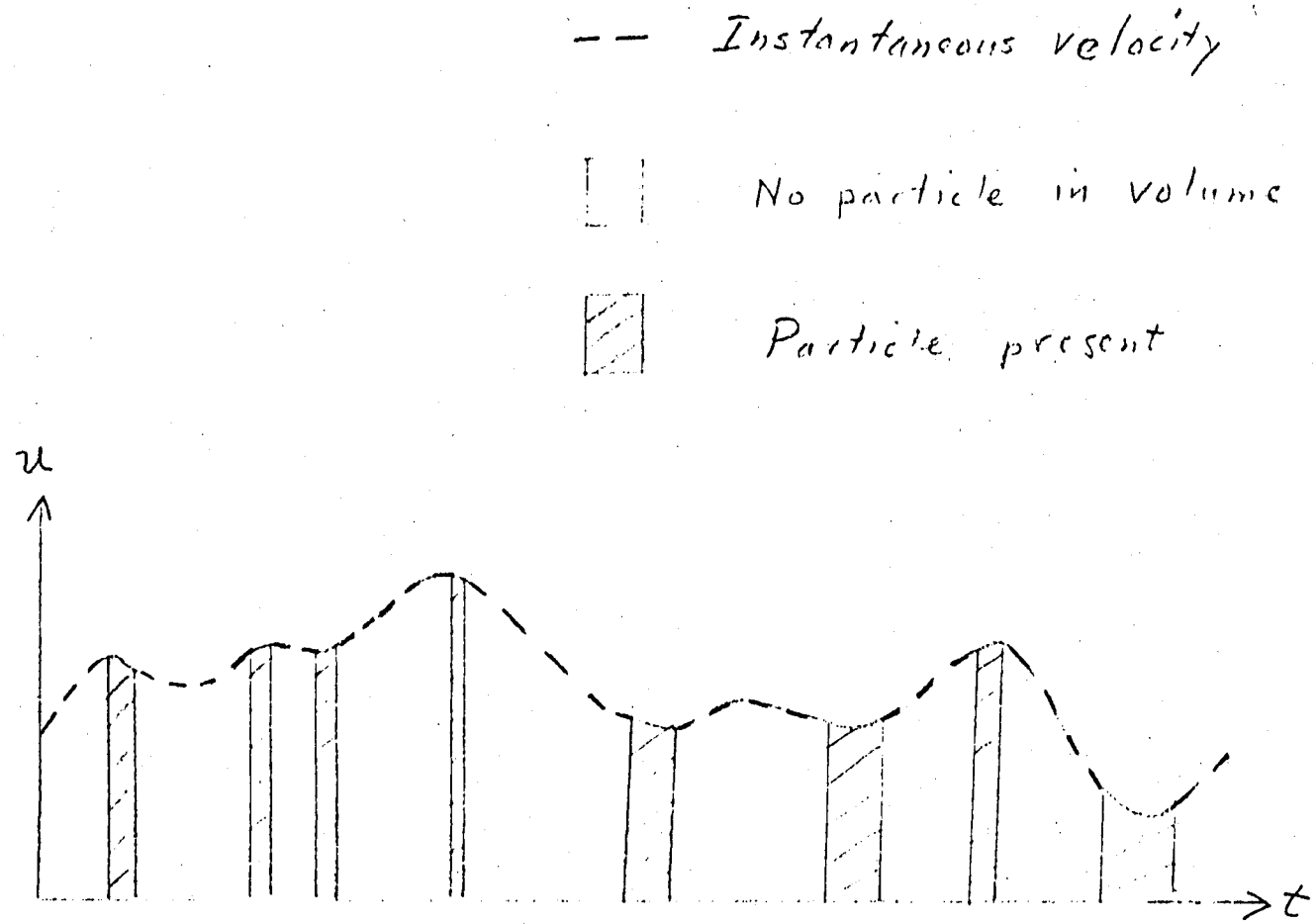
-- Instantaneous velocity
No particle in volume
Particle present
u
t

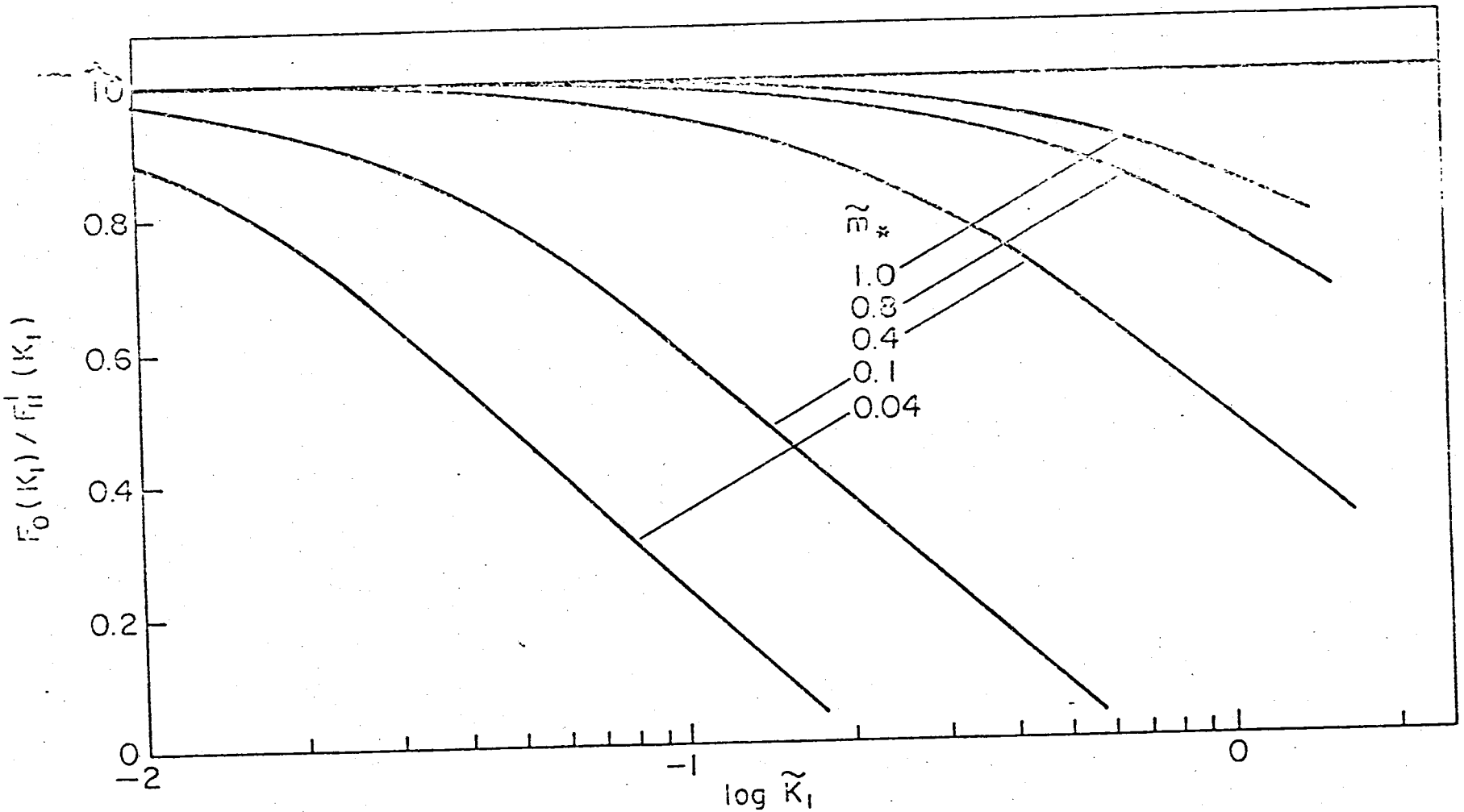
1.0
0.8
0.6
0.4
0.2
0
−2
−1
0
log $\tilde{K}_1$
$F_0(K_1) / F_{II}^1(K_1)$
$\tilde{m}_*$
1.0
0.3
0.4
0.1
0.04

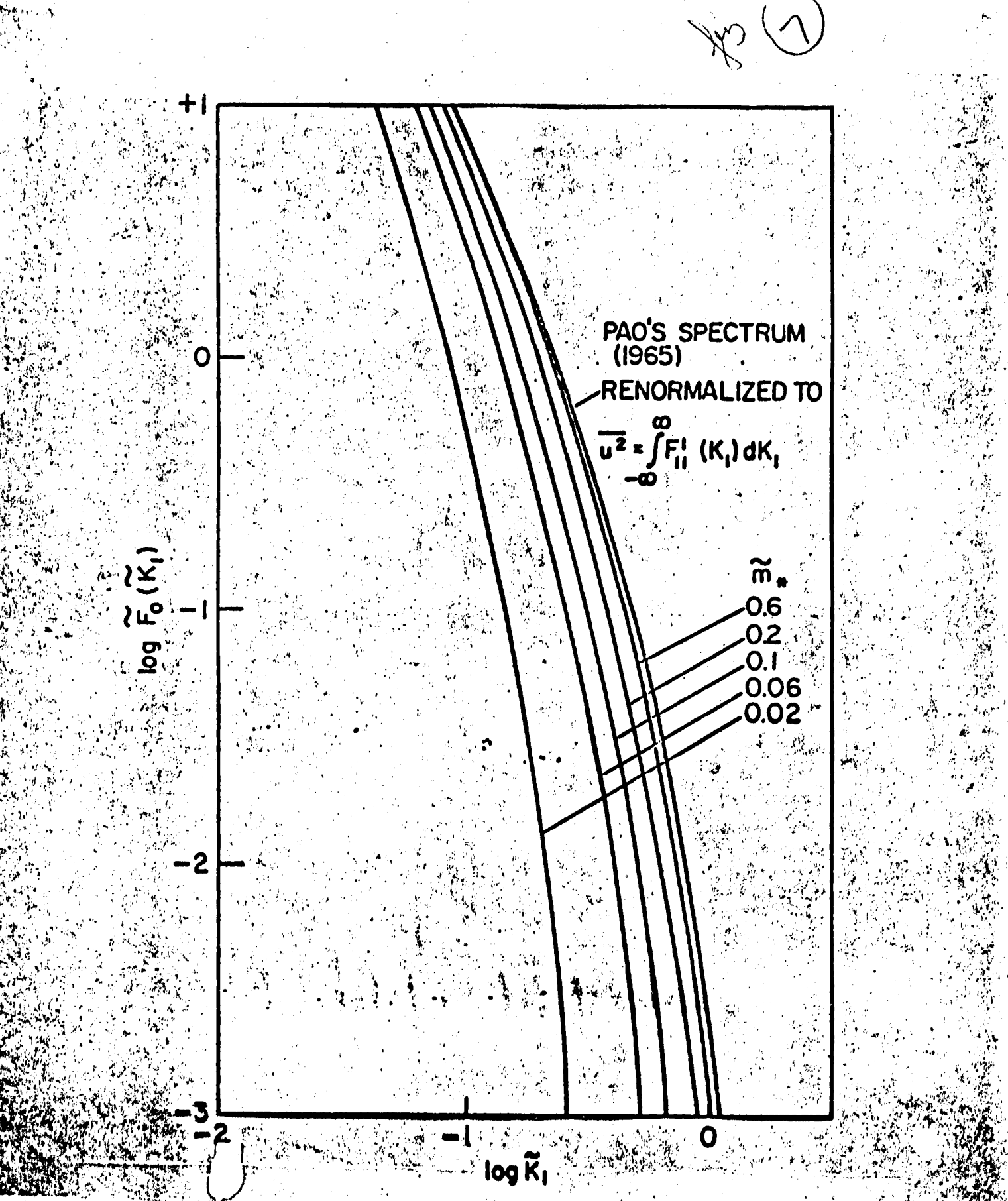
PAO'S SPECTRUM
(1965)
RENORMALIZED TO
$\overline{u^2} = \int_{-\infty}^{\infty} F_{11}'(K_1)\,dK_1$
$\tilde{m}_*$
0.6
0.2
0.1
0.06
0.02
$\log \tilde{F}_0(K_1)$
+1
0
-1
-2
-3
-2
-1
0
$\log \tilde{K}_1$

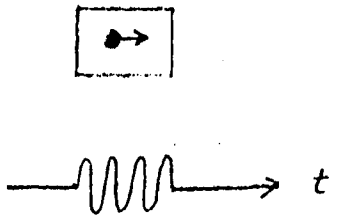

(a)

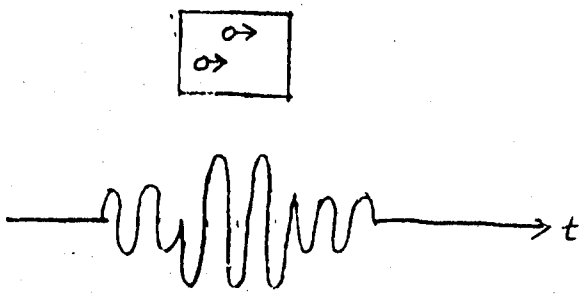

(b)

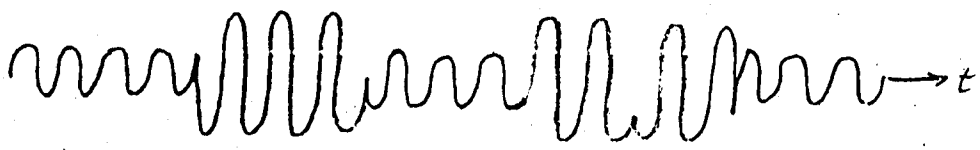

(c)

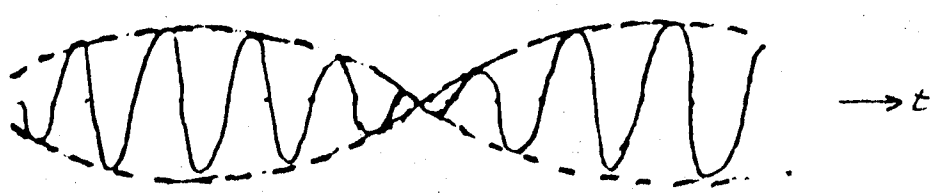

(d)

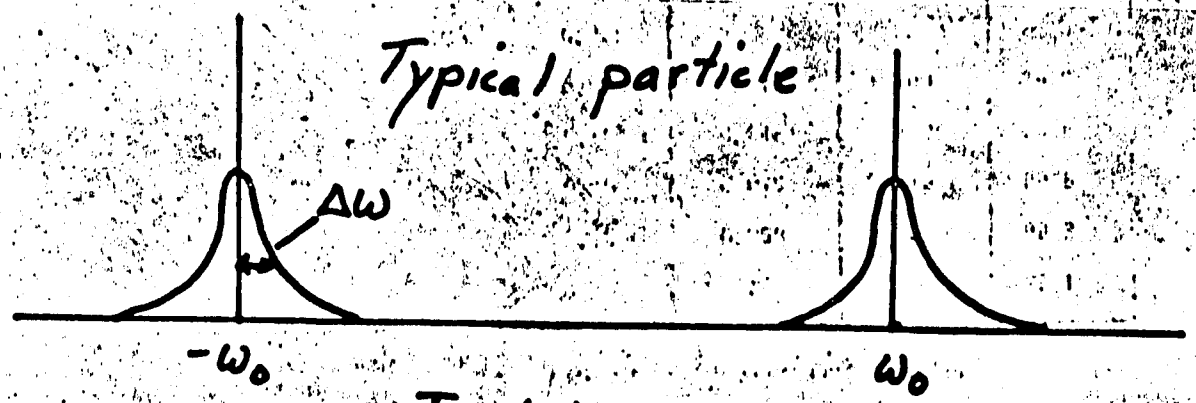

a)

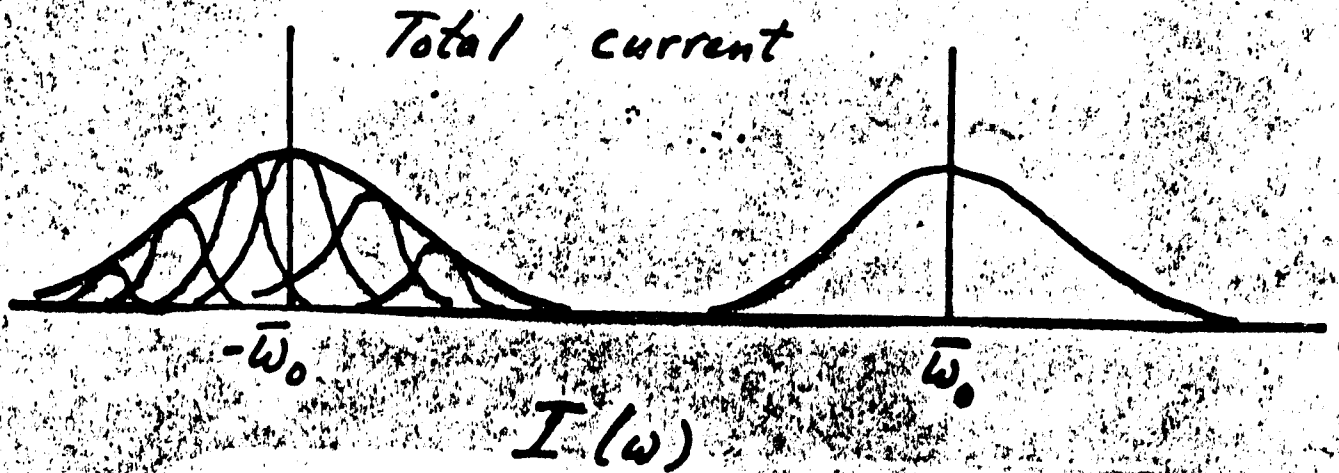

b)

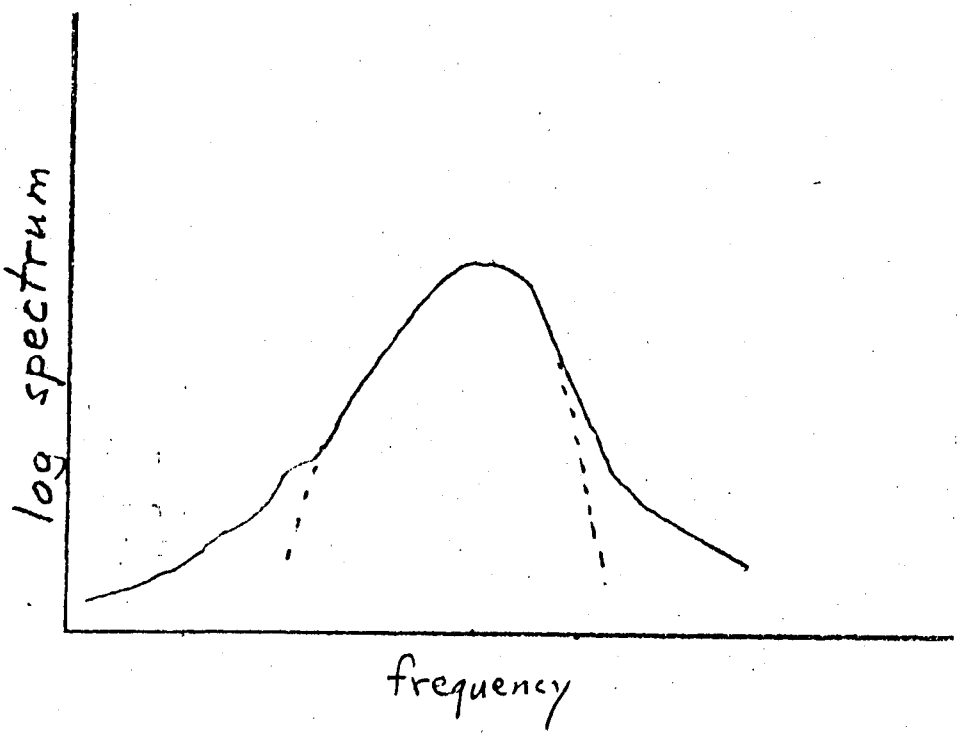
log spectrum
frequency

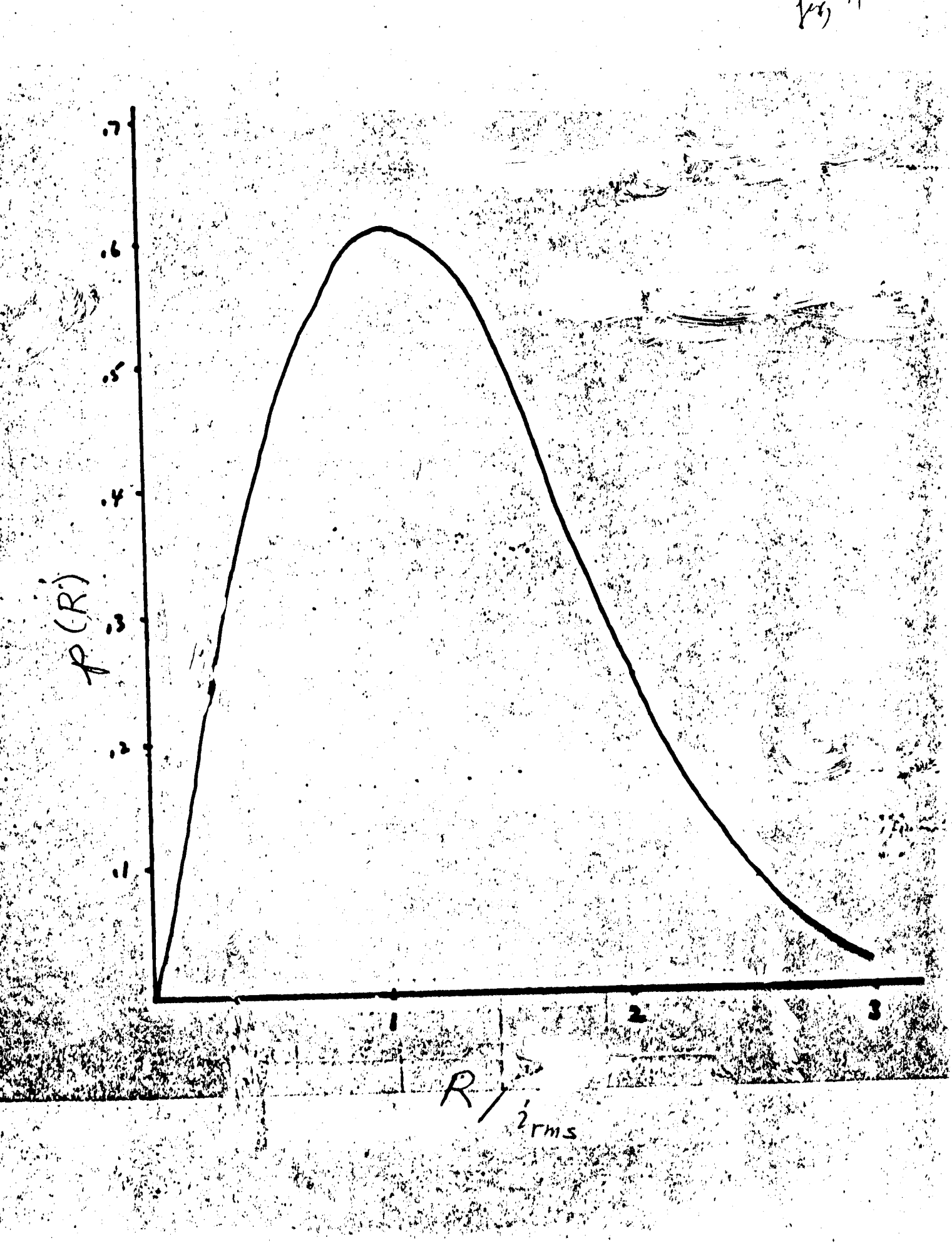
.7
.6
.5
.4
.3
.2
.1
p(R')
1
2
3
R/
i rms

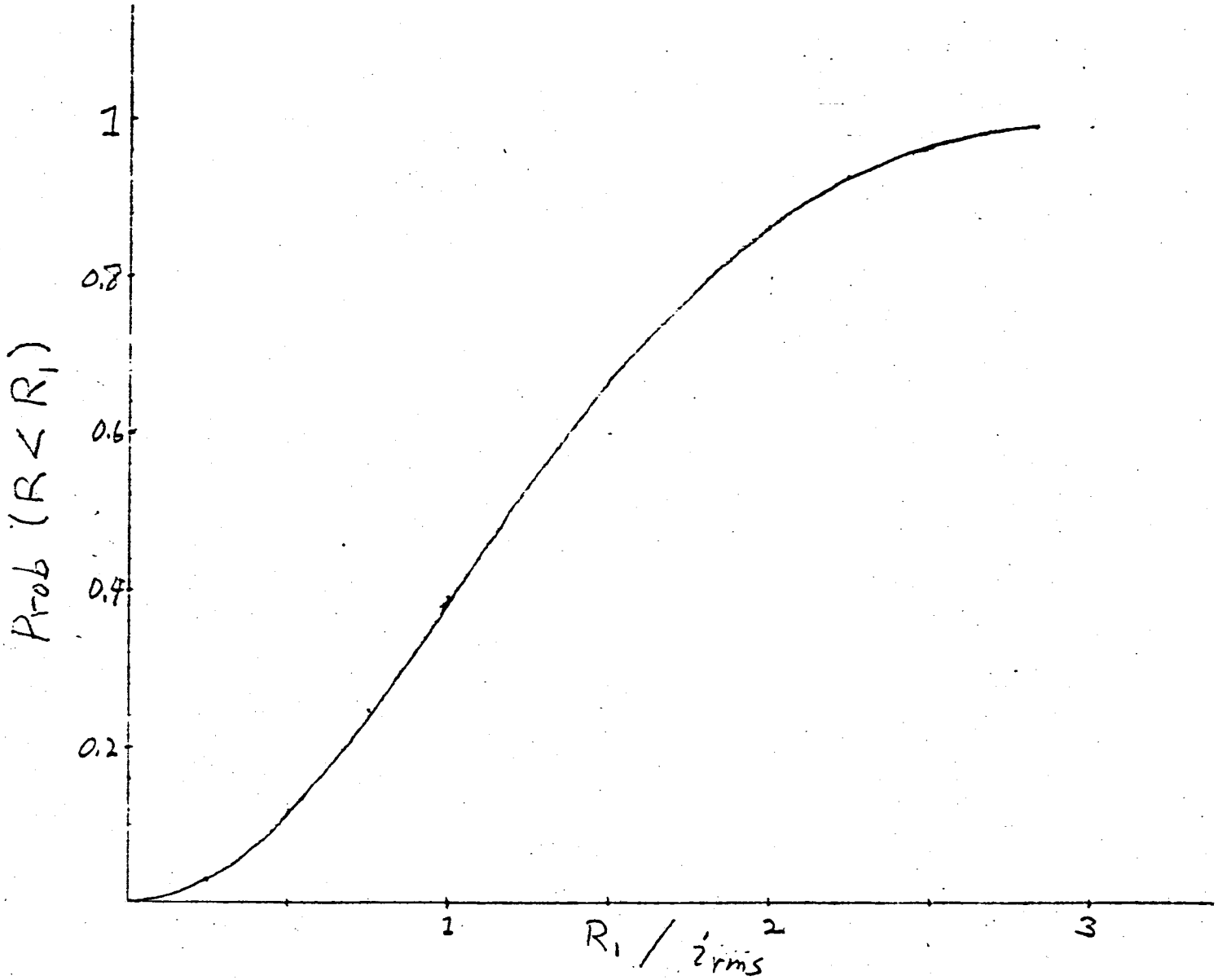
1
0.8
0.6
0.4
0.2
Prob (R < R1)
1
2
3
R1 / σrms

fig 13

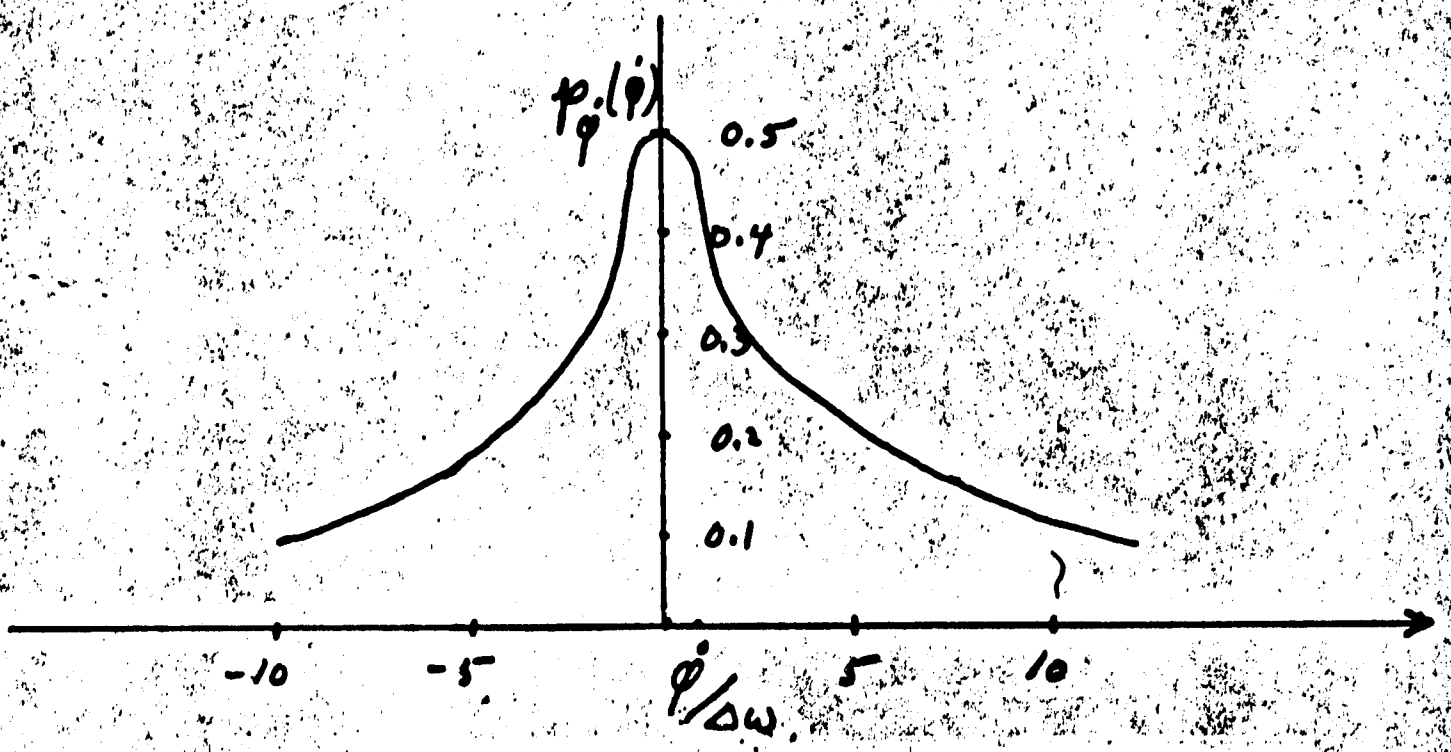
$p_{\varphi}(\dot{\varphi})$
0.5
0.4
0.3
0.2
0.1
-10
-5
5
10
$\dot{\varphi}/\Delta\omega$

Fig 14

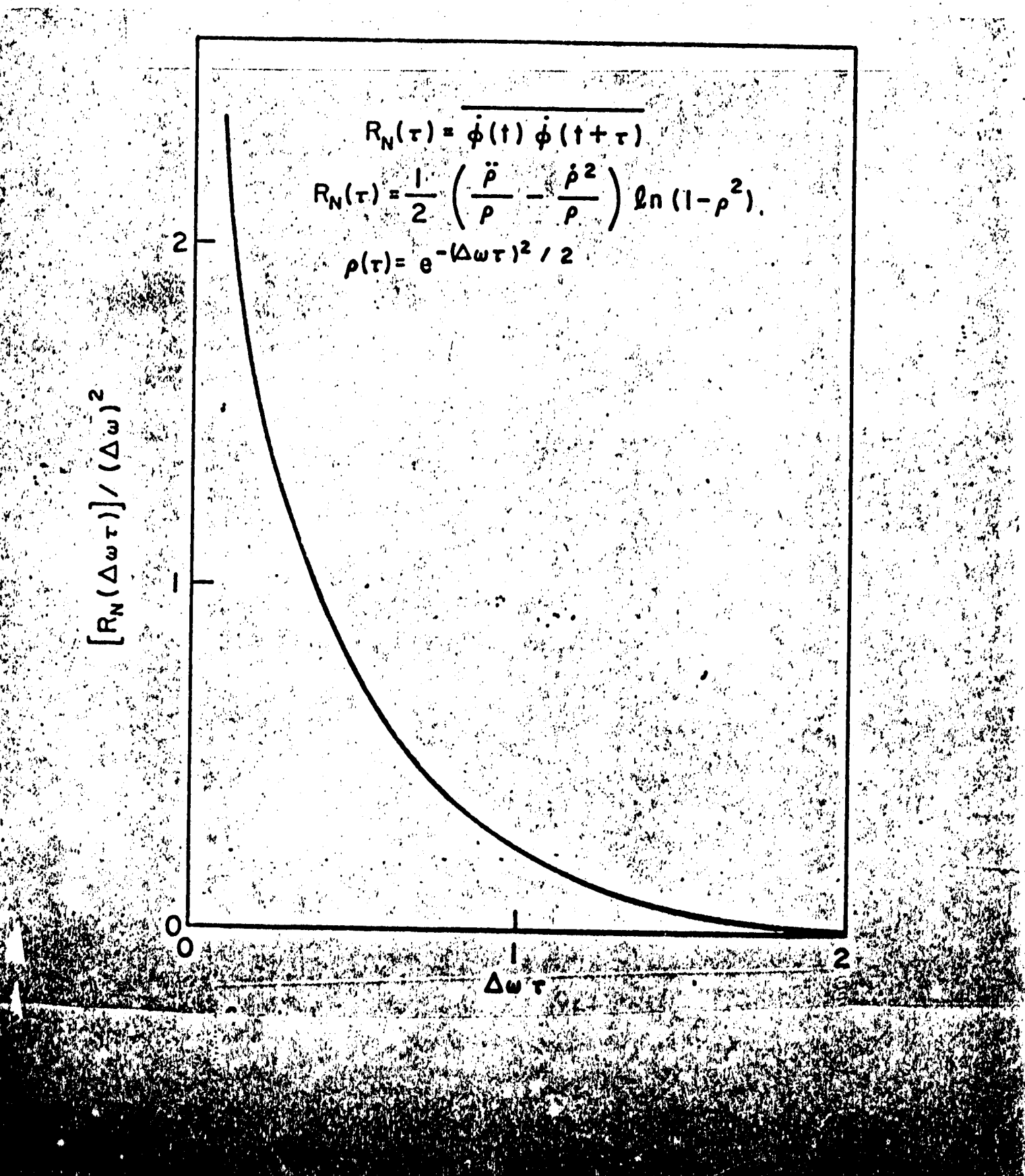
$R_N(\tau) = \overline{\dot{\phi}(t)\,\dot{\phi}(t+\tau)}$
$R_N(\tau) = \frac{1}{2}\left(\frac{\ddot{\rho}}{\rho} - \frac{\dot{\rho}^2}{\rho}\right) \ln(1-\rho^2)$.
$\rho(\tau) = e^{-(\Delta\omega\tau)^2/2}$
$[R_N(\Delta\omega\tau)]/(\Delta\omega)^2$
2
1
0
0
1
2
$\Delta\omega\tau$

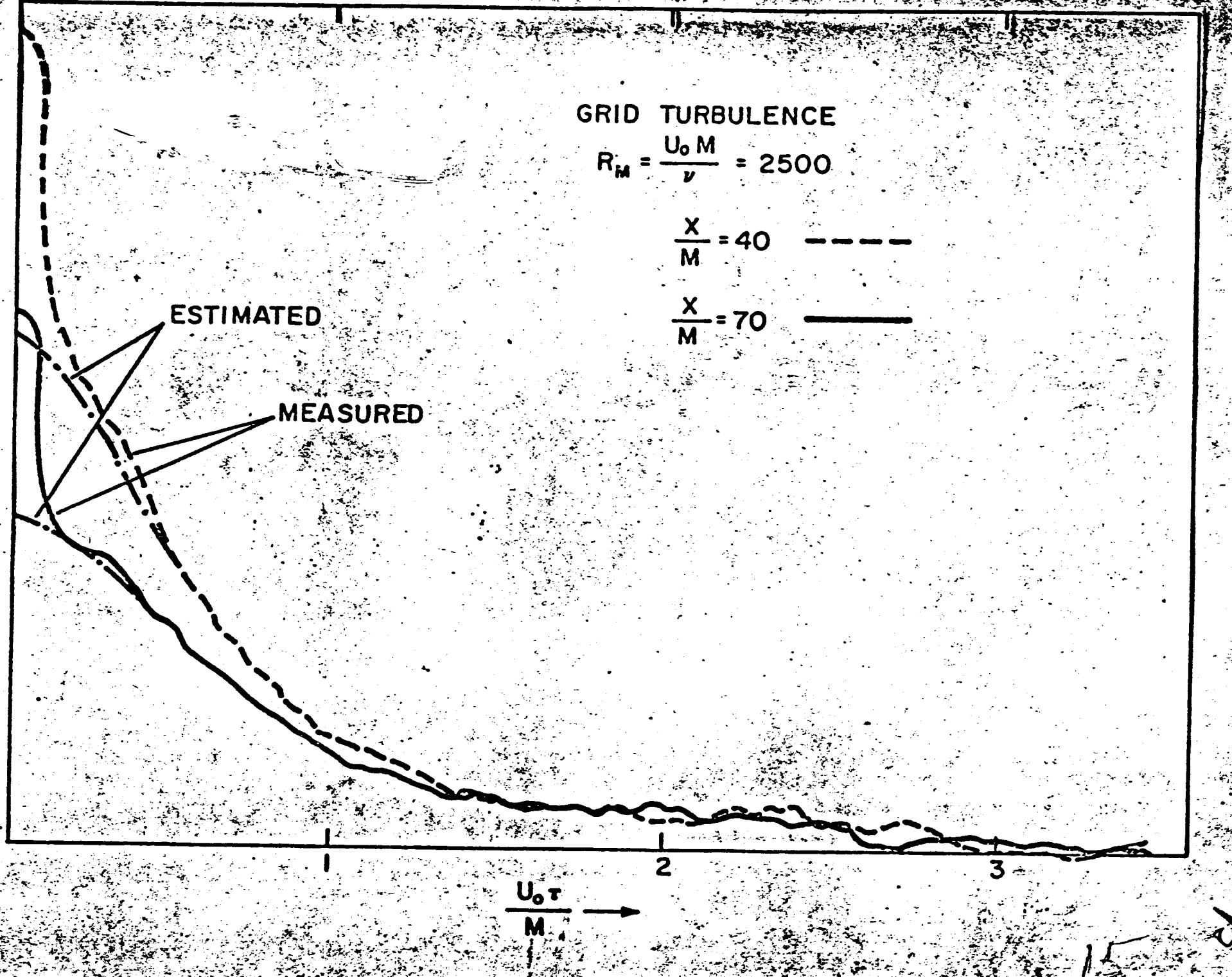
GRID TURBULENCE
$R_M = \frac{U_0 M}{\nu} = 2500$
$\frac{X}{M} = 40$
$\frac{X}{M} = 70$
ESTIMATED
MEASURED
1
2
3
$\frac{U_0 T}{M}$

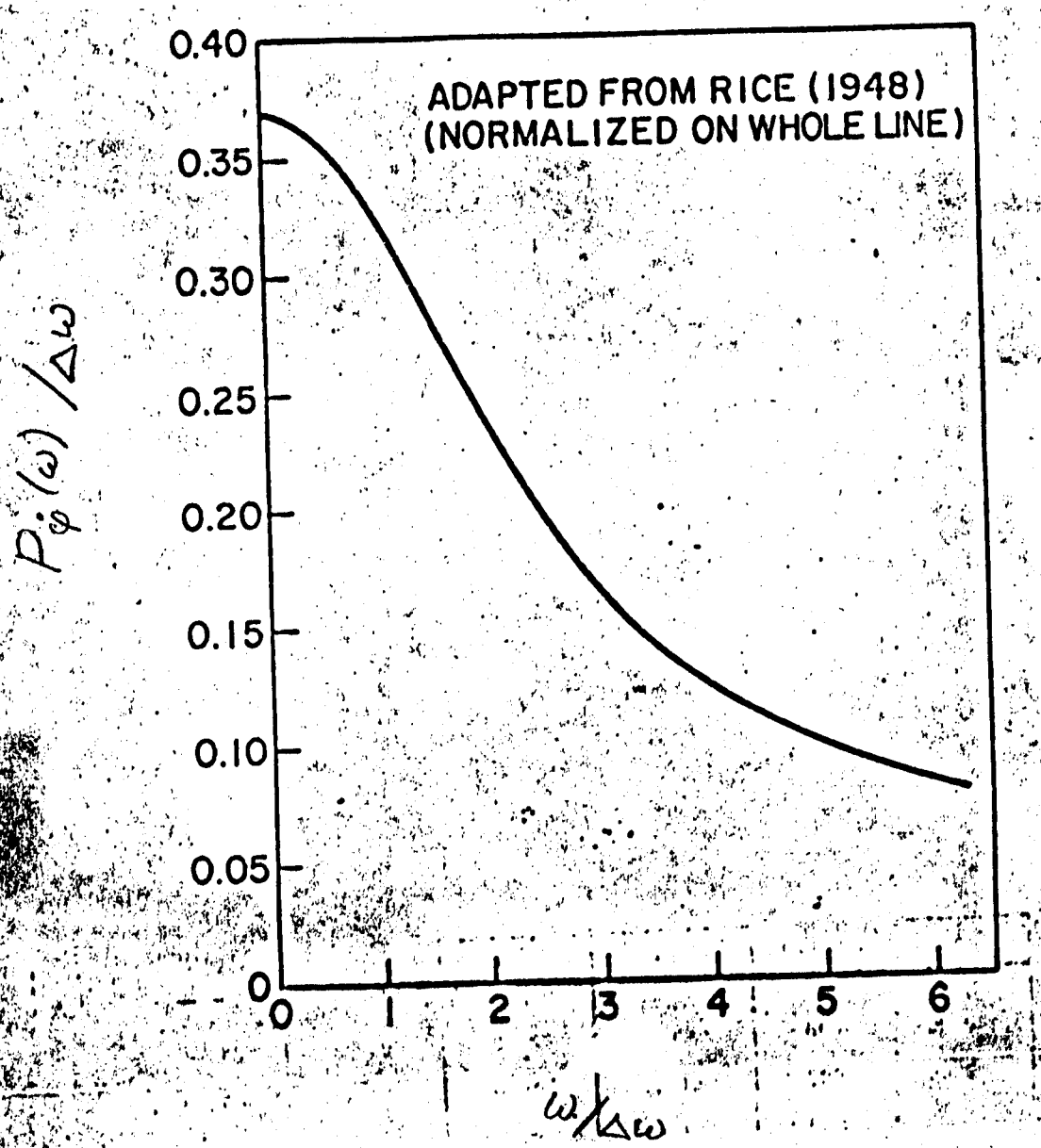
ADAPTED FROM RICE (1948)
(NORMALIZED ON WHOLE LINE)
0.40
0.35
0.30
0.25
0.20
0.15
0.10
0.05
0
0
1
2
3
4
5
6
$P_\phi(\omega)/\Delta\omega$
$\omega/\Delta\omega$

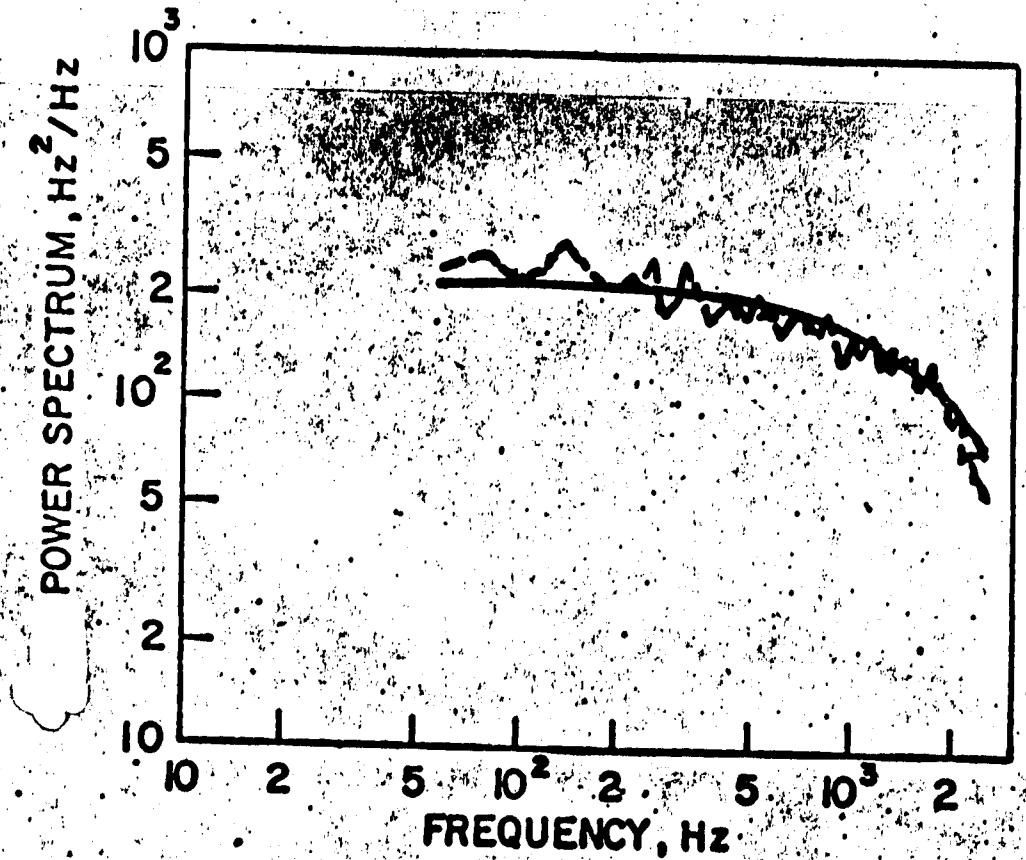
POWER SPECTRUM, Hz²/Hz
10³
5
2
10²
5
2
10
10
2
5
10²
2
5
10³
2
FREQUENCY, Hz

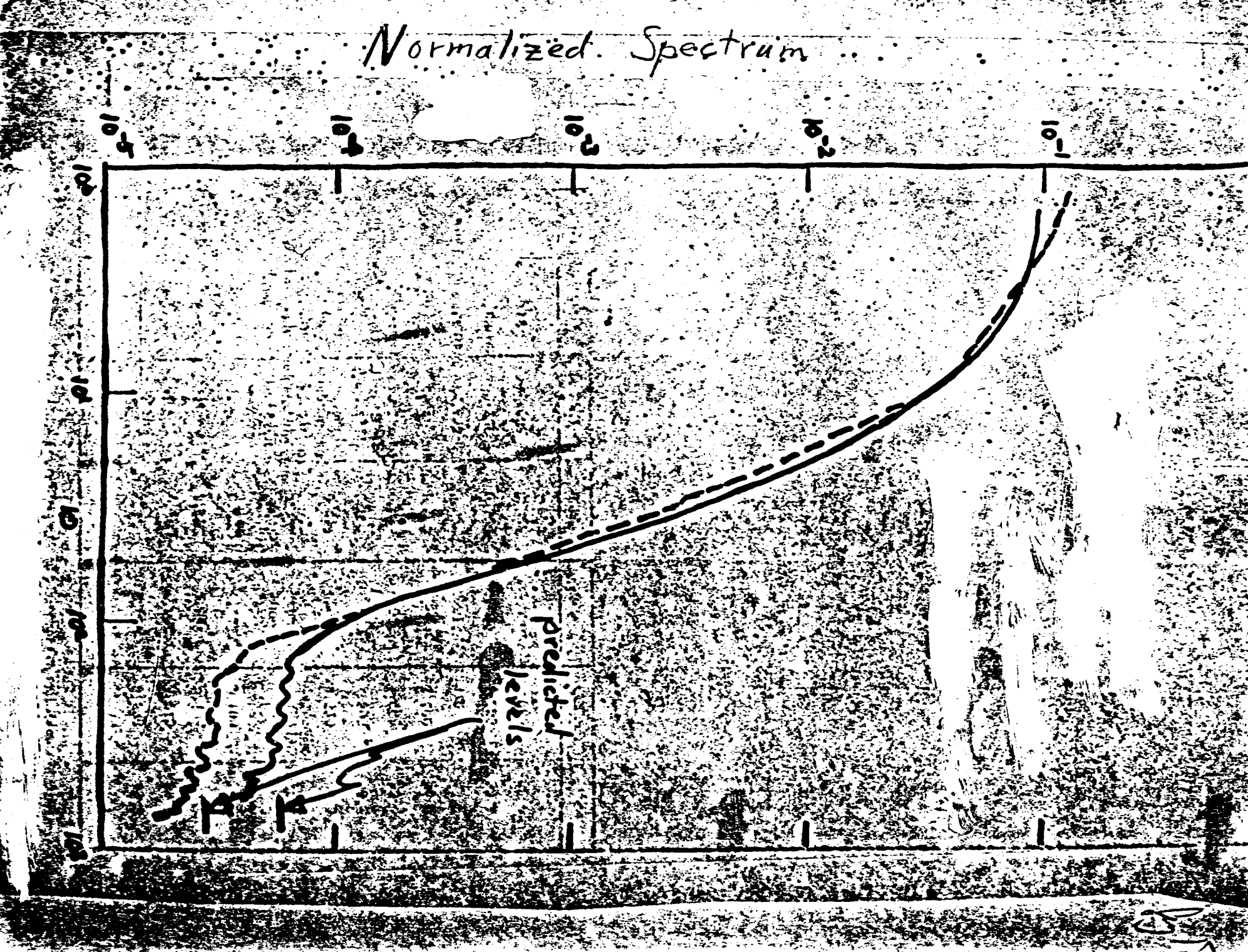
Normalized Spectrum
predicted levels

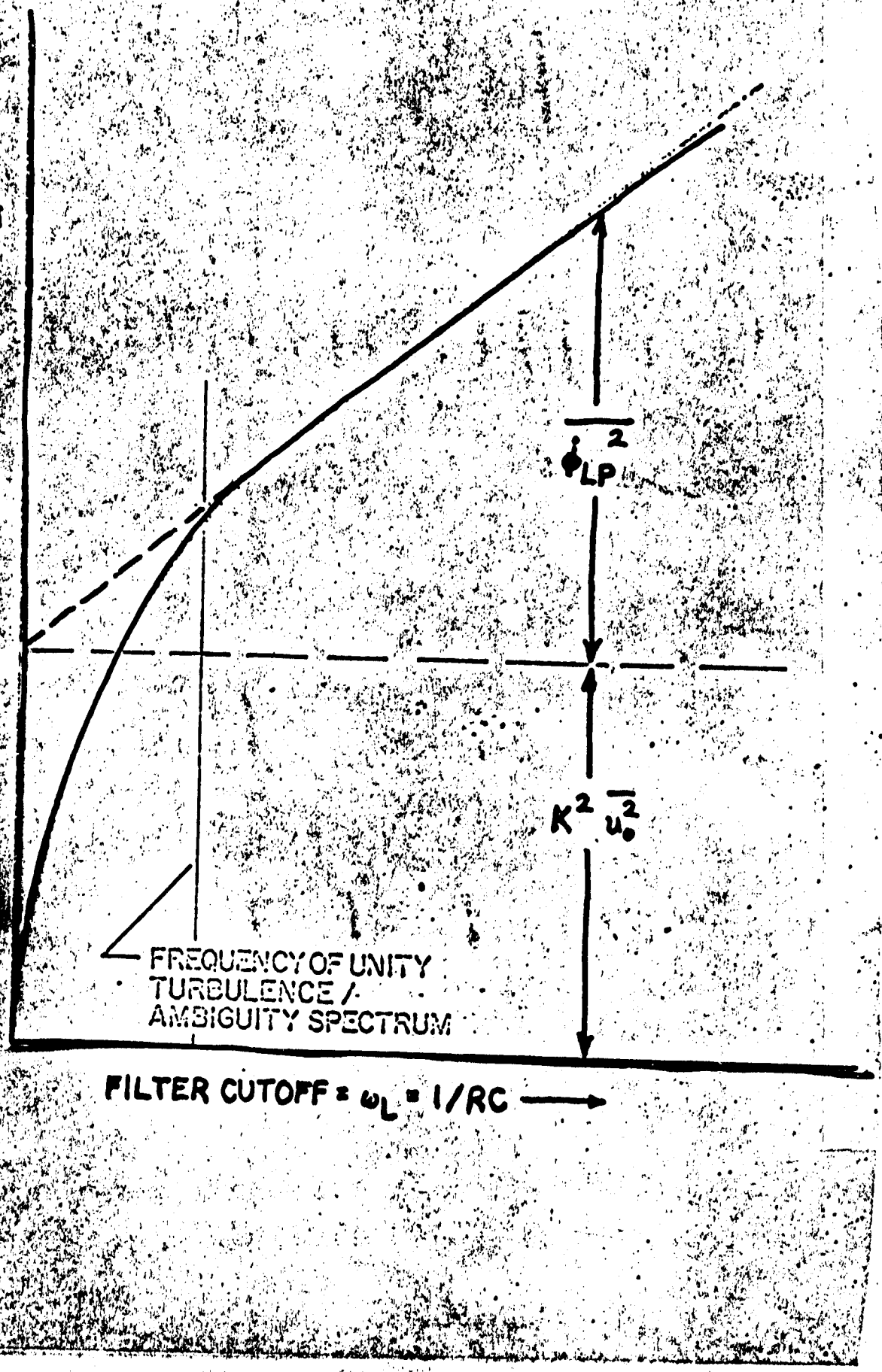
MEAN SQUARE DEMODULATED SIGNAL = $\overline{R^2}$ $\overline{u_0^2}$ + $\overline{\phi_{LP}^2}$
$\overline{\phi_{LP}^2}$
K^2 $\overline{u_0^2}$
FREQUENCY OF UNITY TURBULENCE / AMBIGUITY SPECTRUM
FILTER CUTOFF = ω_L = 1/RC

fig 2b